Title
Regulation of the synaptic trafficking of the vesicular glutamate transporter VGLUT1.

Author
Foss, Sarah

Publication Date
2012

Peer reviewed|Thesis/dissertation

Regulation of the synaptic trafficking of the

vesicular glutamate transporter VGLUT1.

by

Sarah M. Foss

DISSERTATION

Submitted in partial satisfaction of the requirements for the degree of

DOCTOR OF PHILOSOPHY

in

Cell Biology

in the

GRADUATE DIVISION

of the

UNIVERSITY OF CALIFORNIA, SAN FRANCISCO

Acknowledgments

I would first like to thank my mentors: Robert Edwards and Susan Voglmaier. I learned a great deal while completing my thesis research under their excellent guidance. I am also proud to have been Susan's first graduate student (out of hopefully many more to come) and greatly benefited from her excellent hands-on teaching.

I would also like to thank the other members of my thesis committee, Mark von Zastrow and Grae Davis, for their helpful advice and suggestions during many thesis committee meetings. After rotating in both of their labs during my first year, it was great to continue to benefit from their extensive knowledge and expertise.

I would have been unable to complete my research without the help of my fellow members of the Voglmaier lab: Haiyan Li, Magda Santos, Kevin Park, Zachary Schwartz, and Reno Reyes. In particular, I would like to especially thank Haiyan and Magda because anything I didn't learn from Susan, I learned from them. I would also like to thank numerous current and former members of the Edwards lab for their help and suggestions at various points.

In addition, I would like to thank my parents, Dennis and Lora Foss, for their years of support, and for helping to pay for my very expensive undergraduate education and my move to San Francisco.

Finally, I doubt that I would have gotten through grad school without the constant support and love of my husband, Matthew Lohse. Meeting him was by far the best thing to happen in the last seven years.

The experiments described in Chapter 2 were completed by Sarah Foss with the exception of the VGLUT1 vs. -2 comparison (Figure 7) which was done by Haiyan Li, and the design and testing of the knockdown constructs which was completed by Magda Santos. All work was overseen by Susan Voglmaier and Robert Edwards.

The experiments described in Chapters 3 and 4 were completed by Sarah Foss and overseen by Susan Voglmaier and Robert Edwards.

Regulation of the synaptic trafficking of the vesicular glutamate transporter VGLUT1.

Sarah M. Foss

Abstract

Three vesicular glutamate transporters (VGLUT1, -2, and -3) are found in the mammalian central nervous system. The transporters are expressed in different brain regions in synapses with different release properties. Recent work has suggested that the most widely expressed isoforms, VGLUT1 and -2, determine some of the functional properties of their synapses. While the three transporters have very similar transport activity, their synaptic trafficking appears to be differentially regulated and these trafficking differences may account for the observed functional differences.

The main focus of my work has been to identify two additional dileucine-like endocytic motifs in the VGLUT1 N-terminus that can mediate trafficking of the transporter and which are not well-conserved in VGLUT2 or -3. These motifs are in addition to a C-terminal dileucine-like motif that is conserved between the three isoforms. My work also demonstrates that the different dileucine-like motifs utilize different clathrin adaptor proteins with the C-terminal motif using AP-2 and the N-terminal motifs using AP-1. Finally, comparison of VGLUT1 and VGLUT2 demonstrates that VGLUT2 is far more dependent on the conserved C-terminal motif for proper synaptic targeting.

Another line of my research was the identification of novel protein interactors with the two polyproline motifs that are uniquely found in the C-terminus of VGLUT1, downstream of the conserved dileucine-like motif. *In vitro* binding assays identified several intriguing candidates. However, further work is required to determine if these interactions occur *in vivo* and, if so, how they modulate VGLUT1 function.

A final line of research examined whether other putative motifs in the C-terminus of VGLUT1 regulate trafficking of the transporter. While some interesting effects were observed, the functional significance of these motifs remains to be determined.

Table of Contents

List of Tables

List of Figures

Chapter 1. Synaptic Trafficking of VGLUT1.

Chapter 2. Multiple Dileucine-like Motifs Direct VGLUT1 Trafficking.

Chapter 3. Protein Interactions with the C-terminus of VGLUT1.

Chapter 1:

Synaptic Trafficking of VGLUT1.

Glutamate, a key excitatory neurotransmitter, is loaded into synaptic vesicles by a vesicular glutamate transporter (VGLUT). Three VGLUTs (VGLUT1, -2, and -3) are found in the mammalian CNS (H. Omote et al., 2011). VGLUT3 is expressed in a small subset of synapses that are traditionally thought not to be glutamatergic and the transporter plays important roles in hearing and pain perception (R. T. Fremeau, Jr. et al., 2002; C. Gras et al., 2002; M. K. Schafer et al., 2002; R. P. Seal and R. H. Edwards, 2006; R. P. Seal et al., 2008; R. P. Seal et al., 2009). However, the vast majority of glutamatergic synapses utilize either VGLUT1 or -2. These two transporters exhibit a striking, mutually exclusive expression pattern with VGLUT1 expressed in the cortex, hippocampus, and cerebellar cortex while VGLUT2 is found in the thalamus and brainstem (H. Omote et al., 2011). There is also an interesting developmental shift that occurs, at least in mice, two weeks after birth. Before this point, regions that will eventually express VGLUT1 transiently express VGLUT2. Starting around 2 weeks after birth, VGLUT2 expression declines and VGLUT1 expression increases (R. T. Fremeau, Jr. et al., 2004b). Intriguingly, this timing coincides with the point at which mouse pups are a week away from being weaned from their mothers, have newly opened eyes and ears, and are beginning to explore outside their nest. This suggests that the switch from VGLUT2 to VGLUT1 may be due to a requirement for additional complexity in the pups' neural circuits to allow for the encoding of an influx of complex information.

This idea is consistent with the fact that VGLUT1 synapses have a higher potential for plasticity and exhibit less synaptic depression than VGLUT2 expressing synapses (R. T. Fremeau, Jr. et al., 2004a; H. Omote et al., 2011). Recent evidence suggests that these differences are mediated by the transporters themselves NOT the cell

type (R. T. Fremeau, Jr. et al., 2004b; M. C. Weston et al., 2011). However, the transport activity of all VGLUT isoforms is very similar. This is consistent with the fact that there exists a very high degree of homology in the 12 trans-membrane regions of the transporters where the residues critical for glutamate transport likely reside. However, the large cytosolic N- and C-termini are much less conserved (S. Takamori, 2006). The C-terminus of VGLUT1 contains two polyproline motifs (PP1 and PP2) that are not present in VGLUT2 or -3. The more distal motif, PP2, interacts with the endocytic protein endophilin, facilitating VGLUT1 endocytosis under certain conditions (S. De Gois et al., 2006; J. Vinatier et al., 2006; S. M. Voglmaier et al., 2006). Recent work has demonstrated that this interaction is responsible for at least some of the functional differences between VGLUT1 and -2 (M. C. Weston et al., 2011). Thus, the differential trafficking of the VGLUTs underlies their functional diversity.

With regards to VGLUT1 trafficking, prior to beginning my research, a role had been identified for the PP2 polyproline motif and the conserved C-terminal dileucine-like motif. However, no work had been done on the role of the N-terminus in trafficking and nothing was known about the other polyproline motif in VGLUT1's C-terminus, PP2. The C-terminus also contains a potential binding site for a member of the PACS family of adaptor proteins that could allow for indirect binding of clathrin adaptors and trafficking of VGLUT1 independent of a dileucine-like motif. Thus, the goal of the research detailed in following chapters was to further understanding of VGLUT1 trafficking by identification and/or characterization of additional trafficking motifs. This knowledge may be required to fully understand the functional differences between VGLUT1 and other VGLUT isoforms.

References

De Gois S, Jeanclos E, Morris M, Grewal S, Varoqui H, Erickson JD (2006) Identification of endophilins 1 and 3 as selective binding partners for VGLUT1 and their co-localization in neocortical glutamatergic synapses: implications for vesicular glutamate transporter trafficking and excitatory vesicle formation. Cell Mol Neurobiol 26:679-693.

Fremeau RT, Jr., Voglmaier S, Seal RP, Edwards RH (2004a) VGLUTs define subsets of excitatory neurons and suggest novel roles for glutamate. Trends Neurosci 27:98-103.

Fremeau RT, Jr., Kam K, Qureshi T, Johnson J, Copenhagen DR, Storm-Mathisen J, Chaudhry FA, Nicoll RA, Edwards RH (2004b) Vesicular glutamate transporters 1 and 2 target to functionally distinct synaptic release sites. Science 304:1815-1819.

Fremeau RT, Jr., Burman J, Qureshi T, Tran CH, Proctor J, Johnson J, Zhang H, Sulzer D, Copenhagen DR, Storm-Mathisen J, Reimer RJ, Chaudhry FA, Edwards RH (2002) The identification of vesicular glutamate transporter 3 suggests novel modes of signaling by glutamate. Proc Natl Acad Sci U S A 99:14488-14493.

Gras C, Herzog E, Bellenchi GC, Bernard V, Ravassard P, Pohl M, Gasnier B, Giros B, El Mestikawy S (2002) A third vesicular glutamate transporter expressed by cholinergic and serotoninergic neurons. J Neurosci 22:5442-5451.

Omote H, Miyaji T, Juge N, Moriyama Y (2011) Vesicular neurotransmitter transporter: bioenergetics and regulation of glutamate transport. Biochemistry 50:5558-5565.

Schafer MK, Varoqui H, Defamie N, Weihe E, Erickson JD (2002) Molecular cloning and functional identification of mouse vesicular glutamate transporter 3 and its expression in subsets of novel excitatory neurons. J Biol Chem 277:50734-50748.

Seal RP, Edwards RH (2006) The diverse roles of vesicular glutamate transporter 3. Handb Exp Pharmacol:137-150.

Seal RP, Wang X, Guan Y, Raja SN, Woodbury CJ, Basbaum AI, Edwards RH (2009) Injury-induced mechanical hypersensitivity requires C-low threshold mechanoreceptors. Nature 462:651-655.

Seal RP, Akil O, Yi E, Weber CM, Grant L, Yoo J, Clause A, Kandler K, Noebels JL, Glowatzki E, Lustig LR, Edwards RH (2008) Sensorineural deafness and seizures in mice lacking vesicular glutamate transporter 3. Neuron 57:263-275.

Takamori S (2006) VGLUTs: 'exciting' times for glutamatergic research? Neurosci Res 55:343-351.

Vinatier J, Herzog E, Plamont MA, Wojcik SM, Schmidt A, Brose N, Daviet L, El Mestikawy S, Giros B (2006) Interaction between the vesicular glutamate transporter type 1 and endophilin A1, a protein essential for endocytosis. J Neurochem 97:1111-1125.

Voglmaier SM, Kam K, Yang H, Fortin DL, Hua Z, Nicoll RA, Edwards RH (2006) Distinct endocytic pathways control the rate and extent of synaptic vesicle protein recycling. Neuron 51:71-84.

Weston MC, Nehring RB, Wojcik SM, Rosenmund C (2011) Interplay between VGLUT isoforms and endophilin A1 regulates neurotransmitter release and short-term plasticity. Neuron 69:1147-1159.

Chapter 2:

Multiple dileucine-like motifs direct VGLUT1 trafficking.

Multiple dileucine-like motifs direct VGLUT1 trafficking.

Sarah M. Foss[1, 2], Haiyan Li[1], Magda S. Santos[1], Robert H. Edwards[3], and Susan M. Voglmaier[1]*

[1]Department of Psychiatry, [2]Graduate Program in Cell Biology, [3]Departments of Neurology and Physiology, University of California San Francisco, School of Medicine, San Francisco, CA, USA

Abstract

The vesicular glutamate transporters (VGLUTs) package glutamate into synaptic vesicles, and the two principal isoforms VGLUT1 and 2 have been suggested to influence the properties of release. To understand how the VGLUT isoform might influence transmitter release, we have studied their trafficking, and previously identified a dileucine-like endocytic motif in the C-terminus of VGLUT1. Disruption of this motif impairs activity-dependent recycling of VGLUT1, but does not eliminate its endocytosis. We now report the identification of two additional dileucine-like motifs in the N-terminus of VGLUT1 that are not present in the other isoforms. In the absence of all three sequences, VGLUT1 shows limited accumulation at synaptic sites and no longer responds to stimulation. In addition, shRNA-mediated knockdown of clathrin adaptor proteins AP-1 and AP-2 shows that the C-terminal motif acts largely through AP-2 while the N-terminal motifs also utilize AP-1. Without the C-terminal motif, knockdown of AP-1 reduces the amount of VGLUT1 released by stimulation. In contrast to VGLUT1,

the recycling of VGLUT2 depends almost entirely on the conserved C-terminal motif: without this sequence, VGLUT2 redistributes to the plasma membrane. Consistent with these differences, wild type VGLUT1 and VGLUT2 differ in the rate of recycling.

Introduction

The regulated release of neurotransmitter depends on the assembly into synaptic vesicles of membrane proteins that confer regulated exocytotic release. In addition to the proteins that mediate membrane fusion, this process requires the vesicular transporters necessary to fill synaptic vesicles with transmitter. In the case of glutamate, previous work has identified three distinct vesicular glutamate transporters (VGLUTs) ((Y. Aihara et al., 2000; E. E. Bellocchio et al., 2000; S. Takamori et al., 2000; L. Bai et al., 2001; R. T. Fremeau, Jr. et al., 2001; E. Herzog et al., 2001; S. Takamori et al., 2001; R. T. Fremeau, Jr. et al., 2002; C. Gras et al., 2002; M. K. Schafer et al., 2002; S. Takamori et al., 2002)). The three isoforms exhibit similar transport activity *in vitro* but, in general, display mutually exclusive expression patterns in the nervous system (R. T. Fremeau, Jr. et al., 2004a). Surprisingly, the complementary expression of VGLUT1 and -2 correlates with the properties of transmitter release. VGLUT1 is expressed by neuronal populations in the hippocampus, cerebral cortex, and cerebellar cortex that form synapses with a low probability of vesicle release and high potential for plasticity. In contrast, VGLUT2 is expressed by neurons in the thalamus, brainstem, and deep cerebellar nuclei that release transmitter with a higher probability of release at synapses with a lower potential for plasticity ((R. T. Fremeau, Jr. et al., 2004a; H. Omote et al., 2011). Although these

observations originally suggested only a correlation, recent work has raised the possibility that VGLUT1 and -2 can in fact control release probability (M. C. Weston et al., 2011). One corollary of this hypothesis is that the two isoforms differ in their membrane trafficking.

The VGLUTs exhibit a high level of sequence homology in the transmembrane segments that mediate transport, but diverge considerably at the cytoplasmic N- and C-termini that presumably control trafficking. The C-terminus of all three isoforms contains a highly conserved dileucine-like motif that we have previously found important for the endocytosis of VGLUT1 (S. M. Voglmaier et al., 2006). In addition, VGLUT1 contains downstream polyproline domains that interact with the endocytic BAR (Bin/Amphiphysin/Rvs) domain protein endophilin (S. De Gois et al., 2006; J. Vinatier et al., 2006; S. M. Voglmaier et al., 2006). Endophilin recruits VGLUT1 into the faster AP-2-dependent recycling pathway, away from a slower pathway sensitive to brefeldin A, an inhibitor of the AP-1 and -3 adaptors (S. M. Voglmaier et al., 2006). Since VGLUT2 and -3 lack this polyproline motif, the interaction with endophilin may contribute to differences between the isoforms. Recent work has also suggested that the interaction with endophilin contributes to the differences in release probability observed between $VGLUT1^{+}$ and $VGLUT2^{+}$ terminals, although the mechanism remains unclear (M. C. Weston et al.). The role of endophilin in VGLUT1 trafficking also depends on the upstream dileucine-like motif (S. M. Voglmaier et al., 2006).

Although mutagenesis of Phe-510 and Val-511 in the conserved C-terminal dileucine-like motif of VGLUT1 impairs endocytosis, the mutant transporter still undergoes activity-dependent exocytosis and recycling (S. M. Voglmaier et al., 2006).

We now report the identification of additional endocytic motifs in VGLUT1 that are absent in VGLUT2 and find that these contribute to differences in trafficking of the two isoforms.

Materials and Methods

Molecular Biology

Standard PCR directed mutagenesis techniques were used to modify VGLUT1-pH in the pCAGGS vector (S. M. Voglmaier et al., 2006). To generate the FV/GG ΔPP mutant, a stop codon was introduced after Glu-529 to delete the distal C-terminus of VGLUT1-pH (containing both polyproline sequences) and combined with the FV/GG mutation using standard subcloning techniques. ΔC-term VGLUT1-pH was generated by replacement of Ser-504 with a stop codon. ΔN-term VGLUT1-pH was created by replacement of Leu-59 with a start codon, followed by a glutamate residue, to preserve the Kozak sequence (M. Kozak, 1986). ΔN-term & ΔC-term VGLUT1-pH was generated in a similar manner but with Pro-50 replaced by a start codon and glutamate residue. VGLUT2-pH was constructed in a manner similar to VGLUT1-pH with ecliptic pHlourin inserted in the first luminal loop between Gly-107 and Gly-108 of rat VGLUT2 flanked by the same linker sequences used in VGLUT1-pH (S. M. Voglmaier et al., 2006).

RNA interference knockdown

Lentiviral constructs expressing shRNA to rat AP-1γ (AP-1A shRNA: 5'-ACCGAATTAAGAAAGTAGT-3' and AP-1B shRNA: 5'-

GGAATGCTATTCTGTATGA-3') or AP-2μ (5'-GTGGATGCCTTTCGCGTCA-3') (M. Dugast et al., 2005; S. H. Kim and T. A. Ryan, 2009; G. Cheung and M. A. Cousin, 2012) were made in the pFHUBW vector using standard molecular biology procedures. The resulting pFHUBW transfer vectors were co-transfected along with 2 packaging plasmids (pVSV-G and psPAX2) into HEK293T cells using Fugene HD (Promega). Cells were transfected and grown in UltraCULTURE serum-free media (Lonza) supplemented with 1 mM sodium pyruvate, 0.075% sodium bicarbonate, and 2 mM GlutaMax. Approximately 16 h post-transfection, 10 μM sodium butyrate was added to the culture media. Approximately 40 h after transfection, the culture media was collected and viral particles concentrated by centrifugation through a 20% sucrose/PBS-CMF cushion at 80,000 x g for 2 h. Viral particles were resuspended in neuronal culture media supplemented with 4 μg/ml Polybrene (hexadimethrine bromide).

To confirm specific knockdown, rat hippocampal neurons were infected at 7 days *in vitro* (DIV), and harvested at DIV14. Cells were lysed in 100 mM Tris-HCl, pH 7.5, 150 mM NaCl, 1 mM EGTA, and 1% Triton X-100 containing protease inhibitors (1 mg/ml E64, 2 mg/ml aprotinin, 2 mg/ml leupeptin, 2 mg/ml pepstatin, and 20 mg/ml PMSF) and centrifuged at 2,500 x g for 5 min to produce a postnuclear supernatant. For immunoblotting, ~ 25 μg of protein were separated by SDS-PAGE and transferred to PVDF membrane (Immobilon-P, Millipore). AP-1, AP-2 and AP-3 were detected by anti-adaptin γ (1:500, BD Biosciences), anti-adaptin α (1:1000, BD Biosciences), or anti-adaptin δ (1:250, DSHB – University of Iowa), along with appropriate secondary antibodies conjugated to HRP (Jackson ImmunoResearch). Quantifications were performed with ImageJ (http://rsbweb.nih.gov/ij/), using α-tubulin (1:3000, Calbiochem-

EMD) to normalize the signal. To confirm AP-1 knockdown, selected coverslips with cells infected with either AP-1 or vector only lentiviruses, were fixed with 4% PFA in PBS for 20 min after being imaged. Cells were permeabilized and blocked in PBS containing 1% fish skin gelatin, 5% bovine serum albumin, and 0.02% saponin. AP-1 was then detected using anti-adaptin γ (1:200, BD Biosciences) and appropriate secondary antibodies.

Neuronal Culture and Live Cell Imaging

Primary hippocampal neurons were cultured as previously described (H. Li et al., 2011). Briefly, hippocampi were dissected from E19-20 rat pups, dissociated with trypsin, and transfected using the Basic Neuron SCN Nucleofector kit, according to manufacturer's instructions (Lonza). Cells were maintained in Neurobasal media supplemented with 1% heat inactivated fetal bovine serum (FBS), 10% NeuroMix growth supplement (PAA, Dartmouth, MA, USA), 2 mM GlutaMax, 15 mM NaCl, and 10 μg/ml primocin (Lonza). 5-fluoro-2′-deoxyuridine and uridine were added at DIV4–6 to a final concentration of 10 μM in order to limit glial growth. Cells were imaged at DIV14-20 in modified Tyrode's solution (in mM: 126.5 NaCl, 30 dextrose, 2.5 KCl, 2 $CaCl_2$, 2 $MgCl_2$, 10 HEPES) containing 10 μM each of glutamate receptor antagonists 6-cyano-7 nitroquinoxaline-2,3-dione (CNQX) and 3-(2-Carboxypiperazin-4-yl)propyl-1-phosphonic acid (CPP) (Tocris). The total pool size was determined using Tyrode's with 50 mM NH_4Cl (NaCl reduced by 50 mM to compensate). For the knockdown experiments, cells were infected at DIV7 and imaged at DIV14-16.

Cells were imaged as previously described (S. M. Voglmaier et al., 2006; H. Li et al., 2011). Coverslips with transfected neurons were mounted in a perfusion and stimulation chamber (Warner Instruments) on an inverted microscope (Nikon TE3000) fitted with a 63X oil objective. Cells were imaged in modified Tyrode's solution at room temperature with field stimulation (5-10 V/cm) applied using 1 ms bipolar current pulses (A310 Accupulser, WPI). Cells were illuminated using a Xenon lamp (Sutter Instruments) with a 470/40 nm excitation filter and a 525/50 nm emission filter. Images were acquired every 3 s using a QuantEM CCD camera (Photometrics). Metamorph software was used to control data collection and to perform offline analysis. All animal work was conducted under the supervision of the Institutional Animal Care and Use Committee of the University of California, San Francisco. Unless otherwise noted, all chemicals were from Sigma and all tissue culture media from Life Technologies.

Data Analysis

Using Metamorph software, synaptic sites were manually selected by 4 x 4 pixel boxes placed over the center of the boutons. The fluorescence of these regions of interest was averaged and recorded. The average fluorescence of three 4 × 4 pixel boxes without cellular elements was then subtracted as background. To determine the time course of response to stimulation, baseline values from the five frames prior to stimulation were averaged, and the dynamics of fluorescence intensity expressed as fractional change (ΔF) over initial fluorescence (F_0). The data was then normalized to either the peak fluorescence in each trace or the total amount of fluorescence as determined by

application of modified Tyrode's solution containing 50 mM NH_4Cl to alkalinize all synaptic compartments.

To measure the rate of exocytosis and to determine the total amount of transporter exocytosed, cells were imaged in modified Tyrode's medium containing 0.5 - 1 μM bafilomycin A (Calbiochem). The fraction of released transporter was measured as a fraction of the total internal pool, as determined by subtraction of initial fluorescence from fluorescence in the presence of 50 mM NH_4Cl. The size of the readily releasable pool (RRP) was measured with a 100Hz 0.2 s stimulation, followed 1 min later with a 10 Hz for 120 s stimulation to determine the size of the recycling pool (P. Ariel and T. A. Ryan, 2010). The RRP measurement was completed in modified Tyrodes solution with $CaCl_2$ increased to 4 mM. The bath media was replaced with Tyrodes containing 2 mM $CaCl_2$ prior to measuring the recycling pool.

To measure the fraction of transporter on the cell surface, surface fluorescence was quenched with pH 5.5 Tyrode's solution with HEPES replaced by MES. The transporter surface fraction was then calculated by subtracting the average of five frames in pH 5.5 Tyrode's from the average of five frames in standard pH 7.4 Tyrode's solution (both measurements taken prior to stimulation) and divided by the total number of transporters, as determined by fluorescence in the presence of 50 mM NH_4Cl. To quantify the surface level during the stimulation for the mapping the N-terminal motifs (Fig. 2 and 3), the fluorescence at three time points (27 s, 30 s, 33 s) in the middle of stimulation were averaged and this number used instead of the initial fluorescence at pH 7.4. For this data only, four 400 x 400 pixel boxes were placed on each image field,

avoiding cell bodies. Three 4 x 4 pixel boxes were placed in areas in lacking cellular elements to measure the background levels. The fluorescence of these regions was than integrated and background subtracted. To determine the percent decline from peak during stimulation, the fluorescence recorded at 60s (i.e. the last time point of stimulation) was subtracted from peak fluorescence and expressed as a percentage of peak fluorescence.

For all experiments, fluorescence measurements from 20 - 100 boutons per coverslip were averaged and the means from 5 to 31 coverslips from at least two independent cultures were averaged. The one exception is ΔN-term & ΔC-term VGLUT1 in Fig.2 which represents data from 3 coverslips from one culture. Data are presented as means ± SEM. The decay of post-stimulus endocytosis and the fluorescence increase due to stimulation in the presence of bafilomycin were both fit with single exponentials (GraphPad Prism). To determine statistical significance, one-way ANOVA with Tukey's post-test or an unpaired, two-tailed t-test were preformed, as appropriate (GraphPad Prism).

Results

Mutation of the C-terminal dileucine-like motif fails to eliminate VGLUT1 endocytosis

Since replacement of Phe-510 and Val-511 by alanine impairs the endocytosis of VGLUT1 but does not eliminate its synaptic targeting, response to stimulation, or recycling ((S. M. Voglmaier et al., 2006) and Fig.1), we also used glycine replacement

and compared the effect of these mutations in the VGLUT1-pHluorin reporter. Inserted into a lumenal loop of the transporter, the fluorescence of ecliptic pHluorin (a modified form of GFP) is quenched at the low pH of synaptic vesicles (G. Miesenböck et al., 1998; S. Sankaranarayanan and T. A. Ryan, 2000). Exposure to the higher external pH with exocytosis relieves this quenching, and the re-acidification that follows endocytosis again quenches the fluorescence. Changes in fluorescence intensity can thus be used to monitor VGLUT1 exo- and endocytosis. We introduced the F510G/V511G (FV/GG) mutation into the VGLUT1-pHluorin fusion and transfected the resulting construct, along with wild-type (WT) and F510A/V511A (FV/AA) into rat hippocampal neurons. Upon stimulation of these cells rat at 30 Hz for 60 seconds, we found that the FV/GG mutation impairs the compensatory endocytosis of VGLUT1 to a greater extent than the FV/AA mutation (Fig. 1A). After stimulation, endocytosis of the FV/GG mutant (τ_{decay} = 89.4 ± 10.0 s) is significantly slower than WT (τ_{decay} = 36.9 ± 4.3 s; $p < 0.001$) and FV/AA VGLUT1-pH (τ_{decay} = 59.8 ± 5.0 s; $p < 0.05$) (Fig. 1B).

We also used quenching with Tyrode's solution buffered to pH 5.5 with MES to assess the cell surface expression of VGLUT1-pH at steady state, normalizing the results to total synaptic vesicle VGLUT1-pH revealed by alkalinization of the intracellular pool with NH_4Cl. The cell surface fraction of FV/GG VGLUT1-pH (6.0 ± 1.0%) is significantly higher than that of the WT (2.2 ± 0.4%; $p < 0.01$) or FV/AA transporters (3.2 ± 0.7%; $p < 0.05$) (Fig. 1C, solid bars). Three minutes after stimulation, the fluorescence of WT VGLUT1-pH returns to initial levels (WT: 2.3 ± 0.9 s) but a substantial fraction of the mutant transporters (8.2 ± 1.1% for FV/AA and 18.8 ± 1.4%

for FV/GG) remains on the cell surface, quenchable by Tyrode's solution at pH 5.5 (Fig. 1C, striped bars).

Since differences in exocytosis or total synaptic expression of the VGLUT1-pH constructs might have indirect effects on endocytosis, we also examined these properties. The vacuolar H^+-ATPase inhibitor bafilomycin blocks synaptic vesicle reacidification when added to the imaging medium and thus eliminates the contribution of endocytosis to the fluorescence signal, revealing the total amount of transporter that undergoes exocytosis. Stimulating in the presence of bafilomycin and normalizing to the total internal pool of transporter, as revealed by subtraction of the initial fluorescence from the total fluorescence measured with application of NH_4Cl, we observe no significant difference among WT or the mutants in the fraction of transporter that undergoes exocytosis in response to 30 Hz stimulation (WT: 69.6 ± 4.1%; FV/AA: 65.0 ± 2.6%; FV/GG: 65.8 ± 2.2%; $p = 0.31$) (Fig. 1D). In addition, alkalinization of the intracellular pool with NH_4Cl shows no significant differences among the three proteins in total synaptic expression ($p = 0.26$) (Fig. 1E).

These findings demonstrate that glycine mutations specifically disrupt the endocytic role of the dileucine-like motif to a greater extent than alanine substitutions. However, a significant proportion of even the mutant FV/GG VGLUT1 protein still localizes to synapses, responds to stimulation, and undergoes compensatory endocytosis, suggesting additional sorting signals.

The N-terminus of VGLUT1 contains additional endocytosis motifs

To identify additional endocytosis motifs, we produced truncations of either the cytosolic N- or C-terminus of VGLUT1 and examined the effects on behavior of the pHluorin fusion (Fig. 2). We first deleted the two polyproline domains downstream of the dileucine-like motif, including the second which interacts with endophilin (S. De Gois et al., 2006; J. Vinatier et al., 2006; S. M. Voglmaier et al., 2006; M. C. Weston et al., 2011). Replacement of Pro-530 with a stop codon in FV/GG VGLUT1-pH (FV/GG ΔPP) fails to eliminate the increase in fluorescence due to stimulation (from 12.4 ± 2.6% to 43.1 ± 3.1% of total pHluorin) indicating that of the transporter is still largely incorporated in synaptic vesicles (Fig. 2, top row). Since the acidic residues (Glu-505 and -506) upstream of the dileucine-like motif might still bind clathrin adaptor proteins ((D. J. Owen et al., 2004)), we next deleted nearly the entire VGLUT1-pH C-terminus, replacing Ser-504 immediately upstream of the dileucine-like motif with a stop codon (ΔC-term). However, ΔC-term produces no substantial change in steady-state surface level over FV/GG DPP and also fails to eliminate the increase of fluorescence in response to stimulation (from 10.1 ± 1.7% at steady state to 38.1 ± 4.1% of total fluorescence during stimulation).

Deletion of the N-terminus alone (ΔN-term) also fails to eliminate the stimulation-dependent fluorescence, although the magnitude of the change appears to be smaller (from 6.8 ± 0.8% prior to stimulation to 37.1 ± 1.2% of total during stimulation) (Fig. 2). In contrast, VGLUT1-pH lacking both the N- and C-termini (ΔN-term & ΔC-term) resides predominantly on the cell surface (58.4 ± 3.8% of total), widely distributed along the processes rather than concentrated at synaptic sites , and does not respond to

stimulation (fluorescence increases to only 64.1 ± 2.5 % total), indicating that the N-terminus of VGLUT1 contains additional endocytic signals.

The heterotetrameric clathrin adaptor proteins (AP-1, AP-2, AP-3) recognize both tyrosine-based motifs (Yxxϕ, where ϕ is a bulky, hydrophobic residue) and dileucine-like motifs which can also contain acidic residues in the -4 and -5 positions upstream ([DE]xxxL[IL]) ((J. S. Bonifacino and L. M. Traub, 2003)). Inspection of the N-terminal sequence of VGLUT1 reveals two sequences that partially fit the consensus for a dileucine-like motif, $_{6}$EEFRKLA$_{12}$ and $_{22}$LL$_{23}$. The first is atypical since the dileucine portion contains an alanine rather than a larger hydrophobic residue (Iso, Leu, or Met), but mutational analysis of the C-terminal dileucine-like sequence in VGLUT1 shows that alanine can still be recognized (Fig. 1). The second sequence contains of two leucines (L_{22}, L_{23}), but lacks upstream acidic residues (Fig. 3A). Since deletion of the N-terminus alone has only a modest effect on the behavior of VGLUT1-pH, we introduced N-terminal glycine substitutions into ΔC-term VGLUT1-pH. In the first motif, E6G/E7G VGLUT1-pH with the C-terminal deletion (EE/GG ΔC-term) does not replicate the effect of the ΔN-term & ΔC-term double truncation (Fig. 3B). A substantial fraction of the EE/GG ΔC-term mutant is internalized at steady-state (steady-state surface level: 16.6 ± 2.7% of total) and a large increase in fluorescence is observed with stimulation indicating exocytosis (increase to 55.6 ± 1.6% of total). However, addition of L11G/A12G to the EE/GG mutation and ΔC-term (EELA/GGGG ΔC-term) greatly increases steady-state surface expression (47.0 ± 1.9% of total) (Fig. 3B). Stimulation still produces a significant but small increase in fluorescence (to 65.4 ± 1.9% total, $p < 0.0001$).

In the second N-terminal sequence, replacement of Leu-22 and -23 by glycine in ΔC-term VGLUT1-pH (LL/GG ΔC-term) increases steady-state surface expression even further (to 68.5 ± 2.5% total) with no significant fluorescence increase in response to stimulation (73.0 ± 1.8%, $p = 0.16$) (Fig. 3B). Mutation of both $_{11}LA_{12}$ and $_{22}LL_{23}$ motifs in the C-terminal truncation (LALL/GGGG ΔC-term) increases surface expression to similar levels (63.5 ± 3.0%) also with no significant fluorescence increase in response to stimulation (63.1 ± 3.3%, $p = 0.92$). Thus, mutation of either $_{11}LA_{12}$ and $_{22}LL_{23}$ to glycine can mimic the synaptic trafficking defect of the combined ΔN-term & ΔC-term double truncation mutant, indicating that two additional dileucine-like signals are present in the N-terminus of VGLUT1.

N-terminal dileucine-like motifs influence cell surface expression of VGLUT1-pH independent of effects on compensatory endocytosis

To determine an independent role for the N-terminal dileucine-like motifs in trafficking of VGLUT1, we studied the effect of N-terminal mutations with the C-terminal cytoplasmic domain intact. Simultaneous replacement of Glu-6, Glu-7, Leu-11, Ala-12, Leu-22, and Leu-23 with glycine (NT3) (Fig. 4A) increases the surface fraction of VGLUT1-pH (6.3 ± 0.2%) relative to WT (2.1 ± 0.3%) ($p < 0.001$) (Fig. 4B). However, mutation of either the first (NT1) or the second (NT2) dileucine-like motif alone does not increase steady-state cell surface fraction (NT1: 2.5 ± 0.8%; NT2: 2.5 ± 0.5%), and these differences in surface fraction do not reflect differences in protein expression (Fig. 4C).

We then examined the exocytosis of both N- and C-terminal mutants, determining the size of the readily releasable pool (RRP) and recycling pool (RP) as a fraction of the total internal pool of VGLUT1-pH, as measured by subtraction of the initial fluorescence (representing VGLUT1-pH molecules present on the cell surface prior to stimulation) from the total fluorescence as revealed in NH_4Cl. To measure the size of these pools, we evoked release and trapped VGLUT-pH in the alkaline, fluorescent state by blocking acidification with bafilomycin as above (S. Sankaranarayanan and T. A. Ryan, 2000). Eliciting release of docked, primed vesicles in the RRP with 100 Hz for 0.2 s stimulation, we observed no significant differences in the fraction of WT, NT3, or FV/GG VGLUT1-pH released (WT, 5.0 ± 0.8%; NT3, 3.6 ± 0.3%; FV/GG, 4.8 ± 0.8%; $p = 0.24$) (Fig. 4D). Similarly, release of the RP with 10 Hz stimulation for 90 s shows no significant differences (WT, 59.2 ± 2.7%; NT3: 51.4 ± 2.3%; FV/GG: 52.3 ± 3.0%; $p = 0.11$) (Fig. 4D). The rate of exocytosis in response to 10 Hz stimulation also shows no significant differences among the three phenotypes (WT, $\tau = 37.2 \pm 3.7$ s; NT3, $\tau = 45.7 \pm 3.8$ s; FV/GG, $\tau = 46.1 \pm 5.3$ s; $p = 0.28$) (Fig. 4E).

Since the increased steady-state surface level of the N-terminal mutant might reflect a defect in compensatory endocytosis, we examined the endocytosis of VGLUT1 after stimulation at a range of frequencies. Disruption of the N-terminal motifs did not significantly alter the recycling of VGLUT1-pH with stimulation at 5 Hz for 5 min (Fig. 5A), 10 Hz for 1 min (Fig. 5B), 30 Hz for 1 min (Fig. 5C) or 80 Hz for 1 min (Fig. 5D) in contrast to the obvious impairment caused by the C-terminal FV/GG and FV/AA mutations (Fig. 1 and (S. M. Voglmaier et al., 2006).

Although we did not observe a defect in endocytic rate with mutation of the N-terminal motifs alone, the data, taken together, suggests that the N-terminal motifs may mediate the partial endocytosis observed with FV/GG mutation. A substantial portion of the FV/GG VGLUT1 mutant that is released upon stimulation is reinternalized (Fig. 1A, C, D). Consistent with this finding, the low level (~6%) of steady-state surface expression of this mutant (Fig. 1C) supports internalization by some other mechanism and the C-terminus cannot be responsible because ΔC-term also remains largely intracellular and responsive to stimulation (Fig. 2). In addition, endocytosis of ΔC-term is not slower than the FV/GG mutation alone, suggesting that the additional internalization signal is not in the C-terminus (data not shown). Whereas the N-terminal domains may thus partially compensate for loss of the C-terminal dileucine-like motif, the C-terminal dileucine-like motif more fully compensates for loss of the N-terminal motifs. This difference suggested that the N- and C-terminal motifs may promote VGLUT1-pH recycling by different mechanisms.

N- and C-terminal dileucine-like motifs are recognized by different adaptor proteins

To characterize the endocytic mechanisms recruited by the N- and C-terminal motifs, we used previously published shRNA sequences to reduce the levels of the clathrin adaptors AP-1 and AP-2 in hippocampal neurons (M. Dugast et al., 2005; S. H. Kim and T. A. Ryan, 2009; G. Cheung and M. A. Cousin, 2012). Neurons were transfected at the time of plating with WT, FV/GG, or NT3 VGLUT1-pH and infected at 7-8 days *in vitro* (DIV7-8) with lentiviruses expressing constructs containing AP-2μ-, two different AP-1γ-specific shRNA hairpins or an empty vector control along with BFP

to assess infection efficiency. As the only isoform of their subunit in the two adaptors, loss of AP-1γ and AP-2μ destabilizes the other subunits and hence inactivates the entire complex (P. Kantheti et al., 1998; C. Meyer et al., 2000; A. Motley et al., 2003). Western blot analysis of infected hippocampal neurons indeed confirms a specific reduction in the levels of AP-1, but not AP-2 or -3, after infection with virus expressing either of two AP-1 targeted hairpins (Fig. 6A). A similar set of control experiments indicate that the AP-2 shRNA construct (S. H. Kim and T. A. Ryan, 2009) results in a similar reduction in AP-2, but not of AP-1 or AP-3 (data not shown). AP-1 knockdown was also confirmed by immunostaining randomly selected coverslips after live cell imaging (data not shown).

At DIV 14-17, the neurons were stimulated at 30 Hz for 1 min and the fluorescence monitored. Depletion of AP-2 slows the rate of post-stimulus endocytosis of WT VGLUT1 (τ_{decay} = 67.1s ± 8.5 s) relative to the vector control (τ_{decay} = 39.5 ± 4.2 s, $p < 0.05$) (Fig. 6B), consistent with previous work using the same sequence (S. H. Kim and T. A. Ryan, 2009). However, the NT3 shows even more sensitivity to AP-2 knockdown with τ_{decay} = 138.2 ± 19.4 s relative to τ_{decay} = 51.7 ± 5.2 s for control ($p < 0.001$) (Fig. 6C). Since the endocytosis of NT3 depends almost entirely on the C-terminal dileucine-like motif, this suggests that the C-terminal signal depends more strongly on AP-2 than the N-terminal signals. Consistent with this, the post-stimulus endocytosis of FV/GG VGLUT1-pH, which depends primarily on the N-terminal dileucines, was not influenced by AP-2 knockdown (Fig. 6D). AP-2 thus appears more important for VGLUT1 endocytosis mediated by the C-terminal dileucine-like motif, suggesting recognition of the N-terminal motifs by other adaptors.

AP-1 knockdown has different effects on the behavior of VGLUT1-pH. Relative to vector control, knockdown of AP-1γ does not significantly alter the post-stimulus endocytic rate of WT, NT3, or FV/GG VGLUT1-pH (Fig. 6B, C, D). However, the peak level of FV/GG VGLUT1-pH fluorescence reached during stimulation, indicating evoked release, is lower with AP-1 knockdown relative to vector control (Fig. 6C). This effect is specific for FV/GG VGLUT1-pH since AP-1 knockdown has no significant effect on the response to stimulation of either WT or NT3 (Fig. 6B C). Experiments using a second shRNA targeting AP-1γ (AP-1B shRNA) confirm the reduced peak response of FV/GG VGLUT1-pH to stimulation, suggesting that this reduction is not an off-target effect. (Fig. 6D). Quantification of the peak fluorescence as a fraction of the total internal pool of transporters confirms the decrease in response to stimulation (vector: 65.2 ± 1.8%; AP-1A: 55.0 ± 1.6%; AP-1B: 52.7 ± 4.8%; $p < 0.05$ for both comparisons to control) (Fig. 6E). To determine whether the decreased peak fluorescence represents a decrease in exocytosis or an increase in endocytosis during stimulation, we stimulated cells in the presence of the H^+ATPase inhibitor bafilomycin. The fraction of VGLUT1-pH that responds to stimulation at 30 Hz for 1 min stimulation is significantly smaller in cells depleted of AP-1 (vector: 68.3 ± 2.1%; AP-1A: 52.4 ± 3.1%; $p < 0.0006$) (Fig. 6F). Although AP-2 acts through the C-terminal dileucine-like signal to promote the endocytosis of VGLUT2 after stimulation, AP-1 acts through the N-terminal motifs to influence the proportion of VGLUT1 in the recycling pool.

VGLUT1 and VGLUT2 differ in their trafficking

Several lines of evidence have converged to suggest differences in the trafficking of VGLUT1 and 2. Despite the loss of VGLUT1 in knock-out mice, glutamate release persists at hippocampal synapses expressing VGLUT2 but the properties of release differ (R. T. Fremeau, Jr. et al., 2004b; S. M. Wojcik et al., 2004). Reflecting the activity of VGLUT2, the knock-out synapses exhibit increased short-term depression in response to high frequency stimulation compared to the predominantly VGLUT1$^+$ synapses of WT, consistent with a higher release probability at VGLUT2$^+$ than VGLUT1$^+$ synapses. The recent evidence that VGLUT1 and -2 can control release probability further support differences in their trafficking (M. C. Weston et al., 2011). To determine whether VGLUT1 and VGLUT2 do in fact recycle differently, we inserted the ecliptic pHluorin into the large luminal loop of VGLUT2 in a position very similar to the insertion site in VGLUT1 (S. M. Voglmaier et al., 2006). We then compared the response of WT VGLUT1-pH and VGLUT2-pH to stimulation of transfected hippocampal neurons at 40 Hz for 1 min. Although the fluorescence increase in response to stimulation is very similar for VGLUT1 and -2, the kinetics of VGLUT2 recycling appeared slightly different (Fig. 7A). Quantification revealed that the decline from peak fluorescence by the end of stimulation was lower with VGLUT2 (VGLUT1: 55.8 ± 3.2%; VGLUT2: 38.2 ± 2.6% of peak fluorescence; $p < 0.0006$). This dissimilarity could be due to differences in either exo- or endocytosis. However, the fact that rate of post-stimulus endocytosis is slower for VGLUT2, albeit not significantly, suggests the latter (VGLUT1 τ_{decay} = 31.2 ± 1.9 s; VGLUT2 τ_{decay} = 41.9 ± 5.9 s; $p = 0.12$) (Fig. 7A).

The N- and C-terminal sequences of VGLUT1 and VGLUT2 diverge considerably, but VGLUT2 contains the C-terminal dileucine-like motif

($_{512}$SEEKCGFI$_{519}$) conserved in the other VGLUTs. However, the N-terminal dileucine-like motifs of VGLUT1 do not appear to be conserved in VGLUT2. To assess the importance of the C-terminal dileucine-like signal, we replaced Phe-518 and Ile-519 with glycine (FI/GG) and introduced these mutations into VGLUT2-pH, analogous to the FV/GG mutation in VGLUT1. Transfected into neurons, the fluorescence of WT VGLUT2-pH is barely detectable at either pH 7.4 or pH 5.5, but NH_4Cl reveals considerable fluorescence, indicating expression of the protein in an acidic, intracellular compartment (Fig. 7B). In contrast, FI/GG VGLUT2 exhibits substantial steady-state fluorescence at pH 7.4 that is quenched at pH 5.5, indicating mislocalization of the mutant to the plasma membrane. Quantification shows that the FI/GG mutation increases steady-state expression of VGLUT2-pH more than 10 fold (WT, 2.4 ± 0.3%; FI/GG, 29.2 ± 1.8%; $p < 0.0001$), compared to a less than 3-fold increase observed with FV/GG mutation in VGLUT1 (Fig. 1C, 7C). Thus, while VGLUT2 depends almost exclusively on the C-terminal dileucine-like signal for endocytosis and synaptic targeting, VGLUT1 also relies on its N-terminal sequences.

Discussion

Despite the strong conservation of a C-terminal dileucine-like motif in all three VGLUTs, mutation of this motif in VGLUT1 fails to eliminate synaptic targeting and compensatory endocytosis. We now find that the large cytosolic N-terminus of VGLUT1 contains two additional, previously unidentified dileucine-like motifs. Loss of both the N- and C-termini essentially eliminates VGLUT1's synaptic targeting and response to stimulation. Since VGLUT2 and -3 do not contain these N-terminal motifs, they may

contribute to some of the differences observed between the isoforms. However, the question remains as to how these motifs regulate VGLUT1 recycling.

The N-terminal motifs may influence the exo- and/or endocytosis of VGLUT1. However, mutation of these motifs alone fails to alter the rate of VGLUT1 exocytosis in response to 10 Hz stimulation. In addition, the recycling kinetics of VGLUT1, including post-stimulus endocytosis, remain unaltered over a range of stimulation frequencies (5 – 80 Hz). The N-terminal motifs may also influence the size of the readily releasable and/or recycling synaptic vesicle pool of VGLUT1. However, we also find that the size of both pools is unaltered by loss of either the N- or C-terminal motifs.

With regard to endocytosis, the minimal effect of N-terminal mutations reflects redundancy with the C-terminal dileucine-like signal. Indeed, the N-terminus accounts for the residual endocytosis of FV/GG VGLUT1. Evidence for this is the fact that the synaptic targeting observed with ΔC-term VGLUT1 is eliminated by deletion of the N-terminus. Also, compensatory endocytosis of ΔC-term VGLUT1 does not differ in rate from that of FV/GG, excluding a major role for other C-terminal sequences in endocytosis.

Despite the absence of a detectable effect on compensatory endocytosis, mutation of the N-terminal motifs increases by three-fold the amount of transporter present on the cell surface at rest. This effect is only observed when both N-terminal motifs are mutated, suggesting redundancy between them. Although mutation of the C-terminal motif produces a much more substantial defect in compensatory endocytosis after stimulation, it increases steady-state surface expression of VGLUT1 to the same extent. Thus, different mechanisms may regulate steady-state surface expression and

compensatory endocytosis. The results also demonstrate that despite their differences in compensatory endocytosis, either the two N-terminal motifs or the C-terminal motif suffice for trafficking of VGLUT1 to synapses and incorporation into synaptic vesicles.

Mutational analysis of the C-terminal motif also demonstrates that replacement with glycine can have a greater effect on trafficking than alanine. While previous work defining the sequence requirements of myriad membrane proteins for endocytosis has relied almost exclusively on replacement of the dileucine with alanine (J. S. Bonifacino and L. M. Traub, 2003), our results suggest that the endocytic signal remains despite this mutation and previous work has underestimated the importance of these motifs. Persistence of an endocytic signal despite replacement of the dileucine with alanine further indicates that other residues, presumably the conserved residues upstream, can have a primary role in recognition by the adaptor. Consistent with this, the crystal structure of AP-2 binding a peptide containing a dileucine-like motif shows the acidic residue in the -4 position upstream of the dileucine binds a hydrophilic patch composed of residues from the α and σ2 subunits of AP-2 (B. T. Kelly et al., 2008).

shRNA-mediated knockdown of AP-1 and-2 suggests that the N- and C-terminal motifs influence VGLUT1 trafficking through different mechanisms. Knockdown of AP-2 slows the endocytosis of WT VGLUT1-pH but has a much stronger effect on the N-terminal mutant (NT3). Since NT3 VGLUT1-pH relies on the C-terminal motif for endocytosis, this motif must depend primarily on AP-2, consistent with the role for AP-2 and this motif in compensatory endocytosis (J. Dittman and T. A. Ryan, 2009; S. H. Kim and T. A. Ryan, 2009; S. J. Royle and L. Lagnado, 2010). However, AP-2 depletion has no additional effect on FV/GG VGLUT1 endocytosis. Since FV/GG depends on the N-

terminal motifs for internalization, these motifs do not utilize AP-2 or can use alternative adaptors such as AP-1 or -3. Alternatively, the N-terminal motifs may engage an AP-independent mechanism. Indeed, previous work has shown that the impairment of endocytosis with AP-2 depletion can be rescued in part by inhibition of AP-1 and/or -3 with the fungal metabolite brefeldin A (BFA) (S. H. Kim and T. A. Ryan, 2009).

Unlike AP-2, depletion of AP-1 has no effect on WT or NT3 VGLUT1-pH. The C-terminal dileucine motif thus does not interact functionally with AP-1. However, AP-1 knockdown does reduce the peak fluorescence reached during stimulation of FV/GG VGLUT1-pH. Stimulation in the presence of the H^+ATPase inhibitor bafilomycin demonstrates that this reflects a reduction in exocytosis and in particular the size of the recycling pool. Thus, the N-terminal motifs depend on AP-1 for targeting VGLUT1 to the recycling pool.

In contrast to the conserved C-terminal dileucine-like signal, the N-terminal motifs do not appear to be conserved in VGLUT2 or -3. Consistent with this, mutation of the C-terminal motif has a much larger effect on VGLUT2 than VGLUT1: replacement by glycine in VGLUT1 (FV/GG mutation) increases the steady-state cell surface fraction of transporter three-fold, but the analogous mutation (FI/GG) increases surface expression of VGLUT2 ten-fold. VGLUT1 thus relies on multiple endocytic signals and VGLUT2 on only one, predicting differences in the recycling of these proteins at the nerve terminal. Indeed, the analysis of pHluorin fusions shows that the two proteins differ in response to stimulation. During stimulation, when endocytosis begins to reduce the peak fluorescence achieved by exocytosis, VGLUT1-pH shows a more rapid fluorescence decline than VGLUT2-pH, suggesting less efficient retrieval of

VGLUT2 than VGLUT1. Consistent with this, compensatory endocytosis after the stimulus is also faster for VGLUT1 than VGLUT2, and we presume that the additional N-terminal dileucine motifs contribute to the observed difference in endocytic rates.

How do the observed differences in trafficking of VGLUT1 and -2 influence transmitter release? Isoform expression correlates with the probability of release and a direct comparison of VGLUT1^{+} and VGLUT2^{+} synapses using knockout mice has shown differences in short-term plasticity (R. T. Fremeau, Jr. et al., 2004b). More recently, heterologous expression in VGLUT-lacking neurons has shown that the two isoforms can themselves influence the probability of transmitter release, suggesting a direct effect on the release mechanism rather than simply a correlation (M. C. Weston et al., 2011). However, VGLUT1 and -2 exhibit similar transport activity, suggesting that another mechanism must account for the differences in release.

We hypothesize that the role of the VGLUT isoform in glutamate release reflects their targeting to synaptic vesicles with different properties. Previously, we showed that VGLUT1 interacts with the endocytic protein endophilin via a polyproline domain not found in VGLUT2 (S. De Gois et al., 2006; J. Vinatier et al., 2006; S. M. Voglmaier et al., 2006). A mutation that disrupts this interaction converts the properties of release from a VGLUT1^{+} to VGLUT2^{+} synapse (M. C. Weston et al., 2011). However, the effect of the polyproline interaction with endophilin depends on the C-terminal dileucine-like motif (S. M. Voglmaier et al., 2006). In particular, the interaction with endophilin directs VGLUT1 towards an endocytic pathway dependent on the C-terminal dileucine-like motif, and away from one involving AP-1 or -3 (S. M. Voglmaier et al., 2006). Since we now find that the C-terminal dileucine-like motif depends on AP-2 and the N-terminal

motifs on AP-1, the interaction with endophilin appears to influence the endocytic pathway used. Multiple dileucine motifs thus endow VGLUT1 with both the capacity for rapid recycling and the potential for multiple recycling pathways that may in turn contribute to plasticity. In contrast, VGLUT2 relies on a single dileucine-like motif, perhaps accounting for its expression at synapses with lower potential for plasticity as well as its slower recycling.

References

Aihara Y, Mashima H, Onda H, Hisano S, Kasuya H, Hori T, Yamada S, Tomura H, Yamada Y, Inoue I, Kojima I, Takeda J (2000) Molecular cloning of a novel brain-type Na(+)-dependent inorganic phosphate cotransporter. J Neurochem 74:2622-2625.

Ariel P, Ryan TA (2010) Optical mapping of release properties in synapses. Front Neural Circuits 4.

Bai L, Xu H, Collins JF, Ghishan FK (2001) Molecular and functional analysis of a novel neuronal vesicular glutamate transporter. J Biol Chem 276:36764-36769.

Bellocchio EE, Reimer RJ, Fremeau RTJ, Edwards RH (2000) Uptake of glutamate into synaptic vesicles by an inorganic phosphate transporter. Science 289:957-960.

Bonifacino JS, Traub LM (2003) Signals for sorting of transmembrane proteins to endosomes and lysosomes. Annu Rev Biochem 72:395-447.

Cheung G, Cousin MA (2012) Adaptor protein complexes 1 and 3 are essential for generation of synaptic vesicles from activity-dependent bulk endosomes. J Neurosci 32:6014-6023.

De Gois S, Jeanclos E, Morris M, Grewal S, Varoqui H, Erickson JD (2006) Identification of endophilins 1 and 3 as selective binding partners for VGLUT1 and their co-localization in neocortical glutamatergic synapses: implications for vesicular glutamate transporter trafficking and excitatory vesicle formation. Cell Mol Neurobiol 26:679-693.

Dittman J, Ryan TA (2009) Molecular circuitry of endocytosis at nerve terminals. Annu Rev Cell Dev Biol 25:133-160.

Dugast M, Toussaint H, Dousset C, Benaroch P (2005) AP2 clathrin adaptor complex, but not AP1, controls the access of the major histocompatibility complex (MHC) class II to endosomes. J Biol Chem 280:19656-19664.

Fremeau RT, Jr., Voglmaier S, Seal RP, Edwards RH (2004a) VGLUTs define subsets of excitatory neurons and suggest novel roles for glutamate. Trends Neurosci 27:98-103.

Fremeau RT, Jr., Kam K, Qureshi T, Johnson J, Copenhagen DR, Storm-Mathisen J, Chaudhry FA, Nicoll RA, Edwards RH (2004b) Vesicular glutamate transporters 1 and 2 target to functionally distinct synaptic release sites. Science 304:1815-1819.

Fremeau RT, Jr., Troyer MD, Pahner I, Nygaard GO, Tran CH, Reimer RJ, Bellocchio EE, Fortin D, Storm-Mathisen J, Edwards RH (2001) The expression of vesicular

glutamate transporters defines two classes of excitatory synapse. Neuron 31:247-260.

Fremeau RT, Jr., Burman J, Qureshi T, Tran CH, Proctor J, Johnson J, Zhang H, Sulzer D, Copenhagen DR, Storm-Mathisen J, Reimer RJ, Chaudhry FA, Edwards RH (2002) The identification of vesicular glutamate transporter 3 suggests novel modes of signaling by glutamate. Proc Natl Acad Sci U S A 99:14488-14493.

Gras C, Herzog E, Bellenchi GC, Bernard V, Ravassard P, Pohl M, Gasnier B, Giros B, El Mestikawy S (2002) A third vesicular glutamate transporter expressed by cholinergic and serotoninergic neurons. J Neurosci 22:5442-5451.

Herzog E, Bellenchi GC, Gras C, Bernard V, Ravassard P, Bedet C, Gasnier B, Giros B, El Mestikaway S (2001) The existence of a second vesicular glutamate transporter specifies subpopulations of glutamatergic neurons. J Neurosci 21:RC181.

Kantheti P, Qiao X, Diaz ME, Peden AA, Meyer GE, Carskadon SL, Kapfhamer D, Sufalko D, Robinson MS, Noebels JL, Burmeister M (1998) Mutation in AP-3 delta in the mocha mouse links endosomal transport to storage deficiency in platelets, microsomes and synaptic vesicles. Neuron 21:111-122.

Kelly BT, McCoy AJ, Spate K, Miller SE, Evans PR, Honing S, Owen DJ (2008) A structural explanation for the binding of endocytic dileucine motifs by the AP2 complex. Nature 456:976-979.

Kim SH, Ryan TA (2009) Synaptic vesicle recycling at CNS snapses without AP-2. J Neurosci 29:3865-3874.

Kozak M (1986) Point mutations define a sequence flanking at the AUG initiator codon that modulates translation by eukaryotic ribosomes. Cell 44:283-292.

Li H, Foss SM, Dobryy YL, Park CK, Hires SA, Shaner NC, Tsien RY, Osborne LC, Voglmaier SM (2011) Concurrent imaging of synaptic vesicle recycling and calcium dynamics. Front Mol Neurosci 4:34.

Meyer C, Zizioli D, Lausmann S, Eskelinen EL, Hamann J, Saftig P, von Figura K, Schu P (2000) mu1A-adaptin-deficient mice: lethality, loss of AP-1 binding and rerouting of mannose 6-phosphate receptors. EMBO J 19:2193-2203.

Miesenböck G, De Angelis DA, Rothman JE (1998) Visualizing secretion and synaptic transmission with pH-sensitive green fluorescent proteins. Nature 394:192-195.

Motley A, Bright NA, Seaman MN, Robinson MS (2003) Clathrin-mediated endocytosis in AP-2-depleted cells. J Cell Biol 162:909-918.

Omote H, Miyaji T, Juge N, Moriyama Y (2011) Vesicular neurotransmitter transporter: bioenergetics and regulation of glutamate transport. Biochemistry 50:5558-5565.

Owen DJ, Collins BM, Evans PR (2004) Adaptors for clathrin coats: structure and function. Annu Rev Cell Dev Biol 20:153-191.

Royle SJ, Lagnado L (2010) Clathrin-mediated endocytosis at the synaptic terminal: bridging the gap between physiology and molecules. Traffic 11:1489-1497.

Sankaranarayanan S, Ryan TA (2000) Real-time measurements of vesicle-SNARE recycling in synapses of the central nervous system. Nat Cell Biol 2:197-204.

Schafer MK, Varoqui H, Defamie N, Weihe E, Erickson JD (2002) Molecular cloning and functional identification of mouse vesicular glutamate transporter 3 and its expression in subsets of novel excitatory neurons. J Biol Chem 277:50734-50748.

Takamori S, Rhee JS, Rosenmund C, Jahn R (2000) Identification of a vesicular glutamate transporter that defines a glutamatergic phenotype in neurons. Nature 407:189-194.

Takamori S, Rhee JS, Rosenmund C, Jahn R (2001) Identification of differentiation-associated brain-specific phosphate transporter as a second vesicular glutamate transporter. J Neurosci 21:RC182.

Takamori S, Malherbe P, Broger C, Jahn R (2002) Molecular cloning and functional characterization of human vesicular glutamate transporter 3. EMBO Rep 3:798-803.

Vinatier J, Herzog E, Plamont MA, Wojcik SM, Schmidt A, Brose N, Daviet L, El Mestikawy S, Giros B (2006) Interaction between the vesicular glutamate transporter type 1 and endophilin A1, a protein essential for endocytosis. J Neurochem 97:1111-1125.

Voglmaier SM, Kam K, Yang H, Fortin DL, Hua Z, Nicoll RA, Edwards RH (2006) Distinct endocytic pathways control the rate and extent of synaptic vesicle protein recycling. Neuron 51:71-84.

Weston MC, Nehring RB, Wojcik SM, Rosenmund C (2011) Interplay between VGLUT isoforms and endophilin A1 regulates neurotransmitter release and short-term plasticity. Neuron 69:1147-1159.

Wojcik SM, Rhee JS, Herzog E, Sigler A, Jahn R, Takamori S, Brose N, Rosenmund C (2004) An essential role for vesicular glutamate transporter 1 (VGLUT1) in postnatal development and control of quantal size. Proc Natl Acad Sci U S A 101:7158-7163.

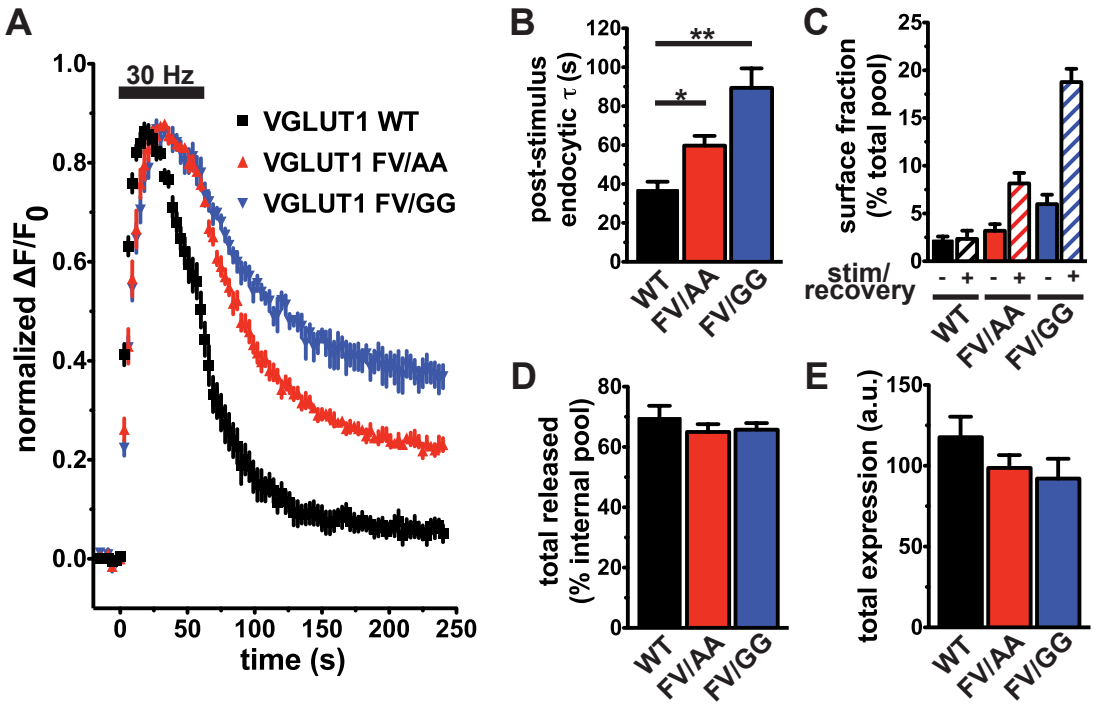
A
30 Hz
VGLUT1 WT
VGLUT1 FV/AA
VGLUT1 FV/GG
normalized ΔF/F0
time (s)
B
post-stimulus endocytic τ (s)
**
*
WT
FV/AA
FV/GG
C
surface fraction (% total pool)
stim/ recovery
D
total released (% internal pool)
E
total expression (a.u.)

Figure 1

Figure 1: ***Mutation of the C-terminal dileucine-like motif slows, but does not eliminate VGLUT1 endocytosis.***

A, Time course of changes in fluorescence intensity ($\Delta F/F_0$) in hippocampal neurons transfected with WT VGLUT1-pH (black), FV/AA VGLUT1-pH (red), or FV/GG VGLUT1-pH (blue). The traces, normalized to peak fluorescence, exhibit increases during stimulation at 30 Hz for 1 min (bar) and decreases after stimulation, consistent with exocytosis followed by endocytosis. Endocytosis of FV/GG VGLUT1-pH is less efficient than either WT or FV/AA.

B, The mean post-stimulus fluorescence decay, fit to a single exponential, is significantly faster for WT (36.9 ± 4.3 s) than FV/AA (59.8 ± 5.0 s; $p<0.05$,*) or FV/GG (89.4 ± 10.0 s; $p < 0.001$,***; one-way ANOVA, Tukey's post-test).

C, The fraction of VGLUT1-pH present on the cell surface at steady-state prior to stimulation (solid bars, stim/recovery –) and 3 min after stimulation (striped bars, stim/recovery +) was estimated by subtracting the value of F/F_0 upon acid quenching with Tyrode's solution containing MES, pH 5.5, from F/F_0 at rest, normalized to total fluorescence upon alkalinization with NH_4Cl. The steady-state surface levels of both FV/AA (3.2 ± 0.7%) and FV/GG (6.0 ± 1.0%) mutants are significantly higher than WT (2.2 ± 0.4%; WT v. FV/AA: $p < 0.01$; WT v. FV/GG: $p < 0.001$; one-way ANOVA, Tukey's post-test). Fluorescence after recovery from stimulation of both FV/AA (8.2 ± 1.1%) and FV/GG (18.8 ± 1.4%) mutants are significantly higher than WT (2.3 ± 0.9%; WT v. FV/AA: $p < 0.01$; WT v. FV/GG: $p < 0.001$; one-way ANOVA, Tukey's post-test).

D, The total amount of transporter released by stimulation at 30 Hz for 1 min stimulus was determined in the presence of bafilomycin. Normalized to total internal pHluorin detected in NH_4Cl, the fraction of WT (69.6 ± 4.1%), FV/AA (65.0 ± 2.6%) and FV/GG VGLUT1-pH released is similar ($p = 0.55$, one-way ANOVA).

E, Total protein expression of WT (117.7 ± 12.7 a.u), FV/AA (98.7 ± 7.9 a.u.), and FV/GG VGLUT1-pH (92.1 ± 12.2 a.u.) at boutons are not significantly different ($p = 0.26$, one-way ANOVA).

Data are the mean ± SEM of > 20 boutons per coverslip from 7-10 coverslips from at least 4 independent cultures.

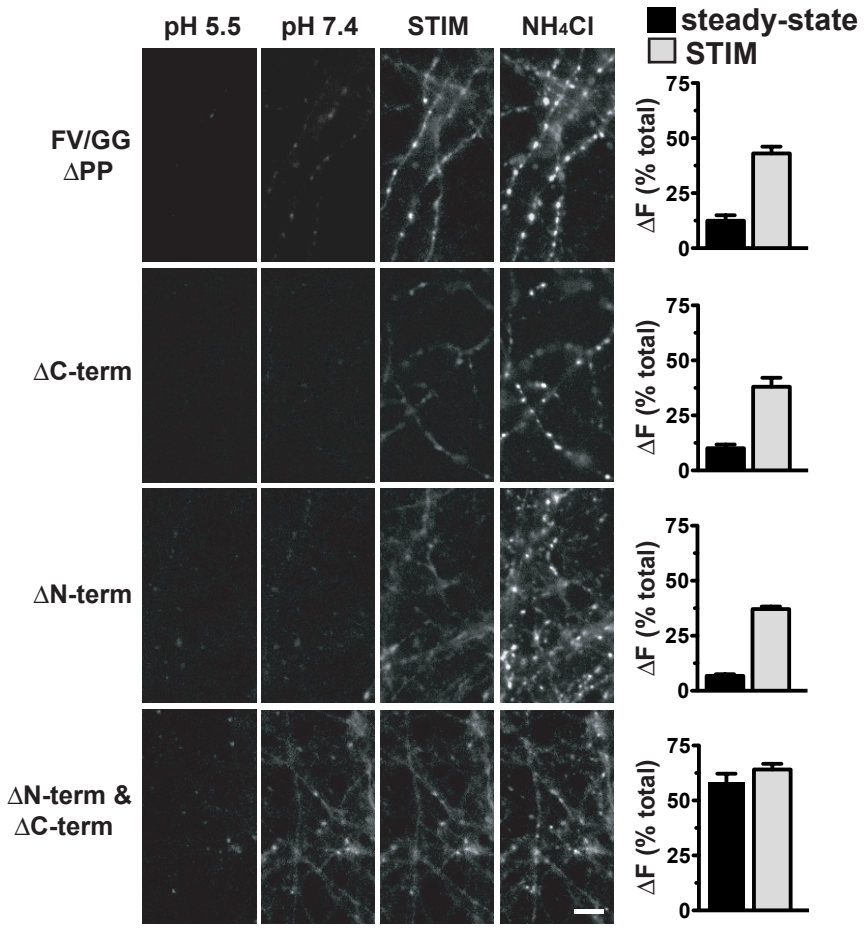
pH 5.5
pH 7.4
STIM
NH4Cl
steady-state
STIM
FV/GG
ΔPP
ΔC-term
ΔN-term
ΔN-term &
ΔC-term
ΔF (% total)
75
50
25
0

Figure 2

Figure 2: VGLUT1 requires either the N- or C-terminus to maintain an intracellular localization.

Hippocampal neurons transfected with VGLUT1-pH truncation mutants were imaged in Tyrode's solution buffered with MES to pH 5.5 to quench surface fluorescence; at rest (pH 7.4); after 30 s stimulation at 30 Hz, near the peak of fluorescence (STIM), and upon alkalinization in 50 mM NH_4Cl to measure total fluorescence. Fluorescence at rest (steady-state, black bars), normalized to unquenched fluorescence at pH 5.5 and total fluorescence, increases during stimulation (STIM, grey bars) in neurons transfected with a VGLUT1-pH mutant that deletes the distal C-terminus (FV/GG ΔPP) (steady-state: 12.4 ± 2.6%; STIM: 43.1 ± 3.1%), a truncation of the full C-terminus (ΔC-term) (steady-state: 10.1 ± 1.7%; STIM: 38.1 ± 4.1%), and a truncation of the full N-terminus (ΔN-term) (steady-state: 6.8 ± 0.8%; STIM: 37.1 ± 1.2%). In contrast, VGLUT1-pH lacking both the N- and C-termini (ΔN-term & ΔC-term) is highly expressed on the cell surface at steady-state (58.4 ± 3.8%), and fluorescence is not significantly increased by stimulation (64.1 ± 2.5%; $p = 0.28$, unpaired, two-tailed t-test). Data represent mean ± SEM of 10-18 coverslips from at least 4 independent cultures with the exception of ΔN-term & ΔC-term (n = 3 coverslips from one culture).

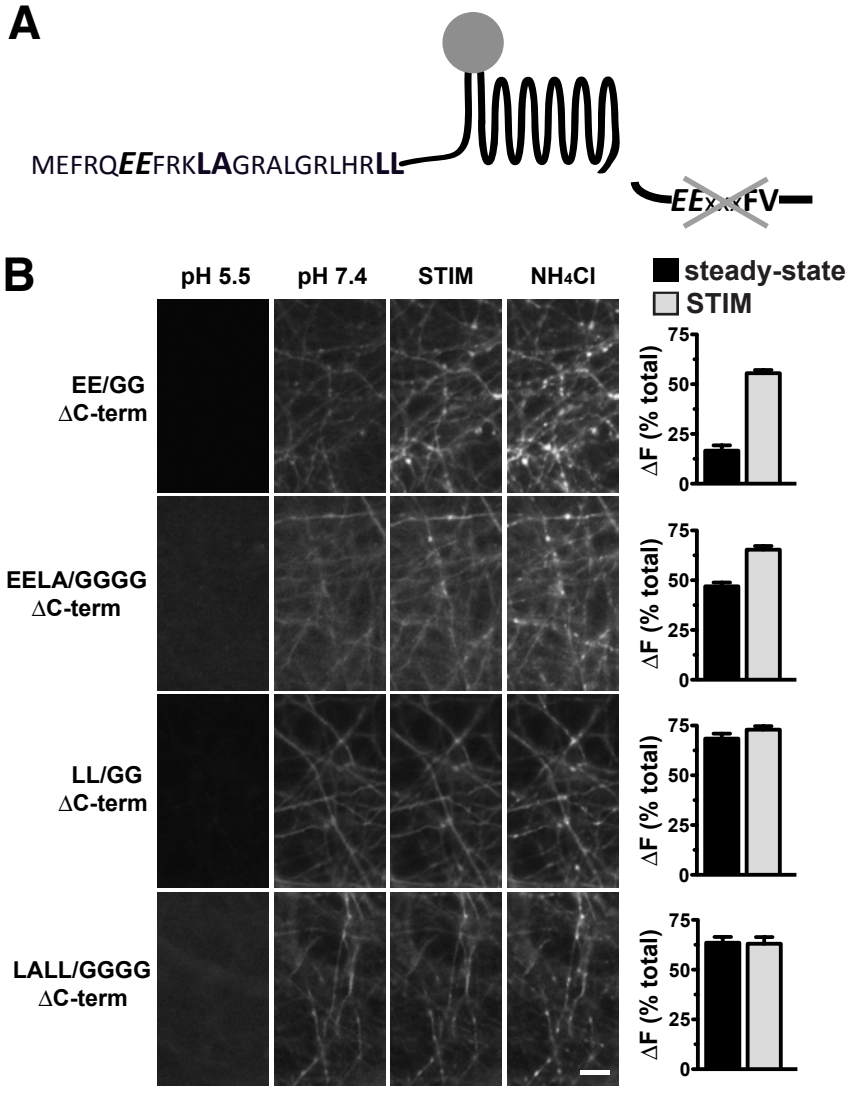
A
MEFRQEEFRKLAGRALGRLHRLL
EExxxFV
B
pH 5.5
pH 7.4
STIM
NH4Cl
steady-state
STIM
EE/GG
ΔC-term
EELA/GGGG
ΔC-term
LL/GG
ΔC-term
LALL/GGGG
ΔC-term
ΔF (% total)
75
50
25
0

Figure 3

Figure 3: The N-terminus of VGLUT1 contains two dileucine-like motifs.

A, Diagram of VGLUT1-pH highlighting the N- and C-termini. Residues in two dileucine-like motifs in the N-terminus that were mutated to glycine in the presence of the full C-terminal deletion are in bold.

B, Point mutations were made in the N-terminus of ΔC-term VGLUT1-pH and constructs transfected into hippocampal neurons were stimulated at 30 Hz for 1 min. Shown are representative fluorescence images of cells in Tyrode's solution buffered with MES to pH 5.5 to quench surface fluorescence; at rest (pH 7.4); after 30 s stimulation, near the peak of fluorescence (STIM), and upon alkalinization in 50 mM NH_4Cl to measure total fluorescence. Fluorescence levels, normalized to unquenched fluorescence at pH 5.5 and total fluorescence, prior to stimulation (black bars) were compared to fluorescence levels after 30 s stimulation (grey bars). Mutation of the acidic residues in the first dileucine-like motif to glycines (EE/GG ΔC-term) does not eliminate the increase in fluorescence in response to stimulation (steady-state: 16.6 ± 2.7%; STIM: 55.6 ± 1.6%). Additional mutation of $_{11}LA_{12}$ (EELA/GG ΔC-term) increases steady-state fluorescence levels (47.0 ± 1.9%), which increase further upon stimulation (STIM: 65.4 ± 1.9%). No fluorescence increase upon stimulation is observed with mutation of $_{22}LL_{23}$ (LL/GG ΔC-term) (steady-state: 68.5 ± 2.5%; STIM: 73.0 ± 1.8%) or with mutation of both $_{22}LL_{23}$ and $_{11}LA_{12}$ (LALL/GGGG ΔC-term; steady-state: 63.5 ± 3.0%; STIM: 63.1 ± 3.3%). All data mean ± SEM of 8-10 coverslips from 2 independent cultures.

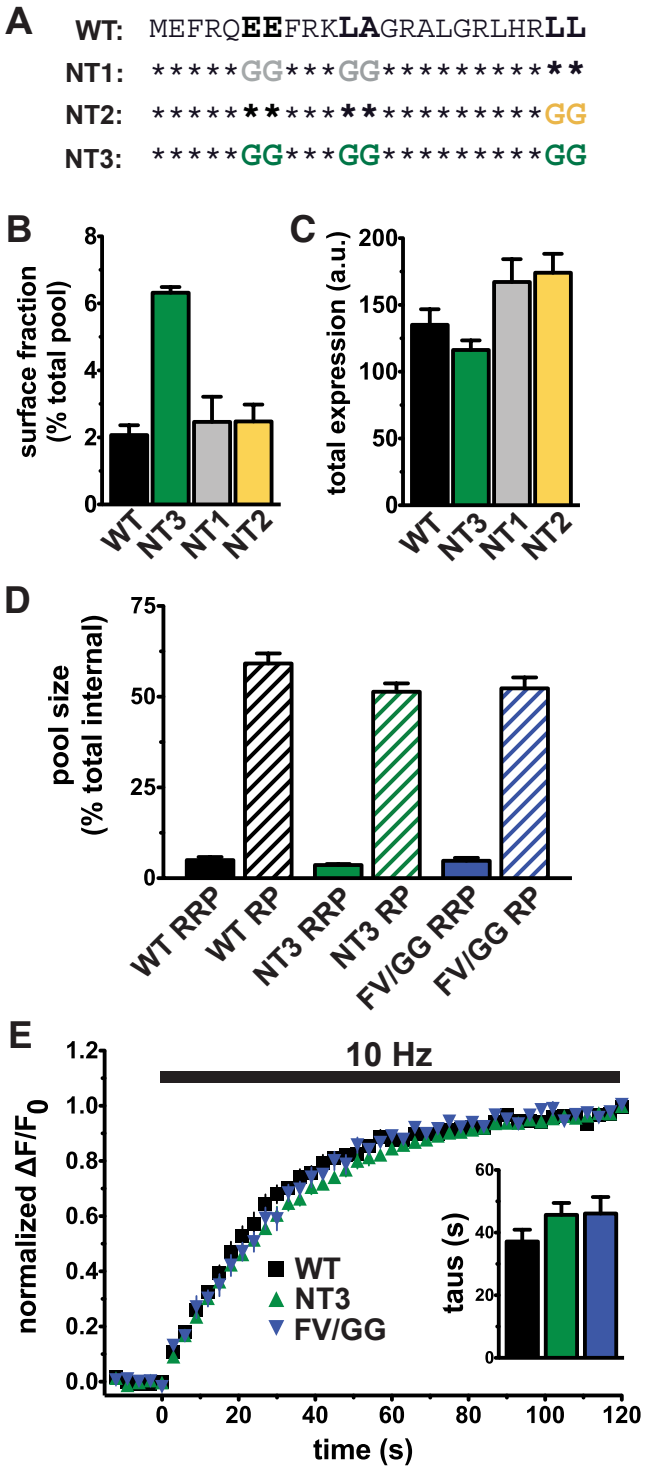
A
WT: MEFRQEEFRKLAGRALGRLHRLL
NT1: *****GG***GG**********
NT2: ******************GG
NT3: *****GG***GG*********GG
B
surface fraction (% total pool)
WT
NT3
NT1
NT2
C
total expression (a.u.)
WT
NT3
NT1
NT2
D
pool size (% total internal)
WT RRP
WT RP
NT3 RRP
NT3 RP
FV/GG RRP
FV/GG RP
E
10 Hz
normalized ΔF/F0
time (s)
WT
NT3
FV/GG
taus (s)

Figure 4

Figure 4: Mutation of N-terminal dileucine-like motifs increases cell surface expression.

A, To disrupt the first N-terminal dileucine-like motif of VGLUT1-pH, Glu-6, -7, Leu-11, Ala-12 were replaced with glycine (NT1). Leu-22 and -23 were replaced to eliminate the second motif (NT2). Mutation of all six residues disrupts both N-terminal motfis (NT3).

B, The surface fraction of NT3 (6.3 ± 0.2%) is significantly higher than either WT (2.1 ± 0.3%, $p < 0.001$) or either individual N-terminal mutants, NT1 (2.5 ± 0.8%, $p < 0.01$) or NT2 (2.5 ± 0.5%, $p < 0.01$) (one-way ANOVA, Tukey's post-test).

C, Total expression level of NT1 (116.3 ± 7.2 a.u., $p > 0.05$), NT2 (167.2 ± 17.1 a.u., $p > 0.05$), and NT3 (174.2 ± 14.2 a.u., $p > 0.05$) are not different than WT (135.1 ± 11.7 a.u.) (one-way ANOVA, Tukey's post-test).

D, The size of the readily releasable pool, as measured with a 100 Hz 200 ms stimulus, is not significantly altered by mutation of either the N- or C-terminal dileucine-like motifs (WT: 5.0 ± 0.8% ; NT3: 3.6 ± 0.3%; FV/GG: 4.8 ± 0.8%; $p = 0.24$, one-way ANOVA). Recycling pool size, as measured by a 10 Hz 90 s stimulus, is also not significantly different for WT (59.2 ± 2.7%), NT3 (51.4 ± 2.3%), and FV/GG (52.3 ± 3.0%; $p = 0.11$, one-way ANOVA).

E, The rate of exocytosis in response to a 10 Hz 120s stimulus is not significantly different between WT (black, τ_{growth} =37.2 ± 3.7 s), NT3 (green, τ_{growth} = 45.7 ± 3.8 s), and FV/GG (blue, τ_{growth} = 46.1 ± 5.3 s; $p = 0.28$, one-way ANOVA).

All data mean ± SEM of 8-31 coverslips from at least 3 independent cultures with > 20 synapses averaged per coverslip.

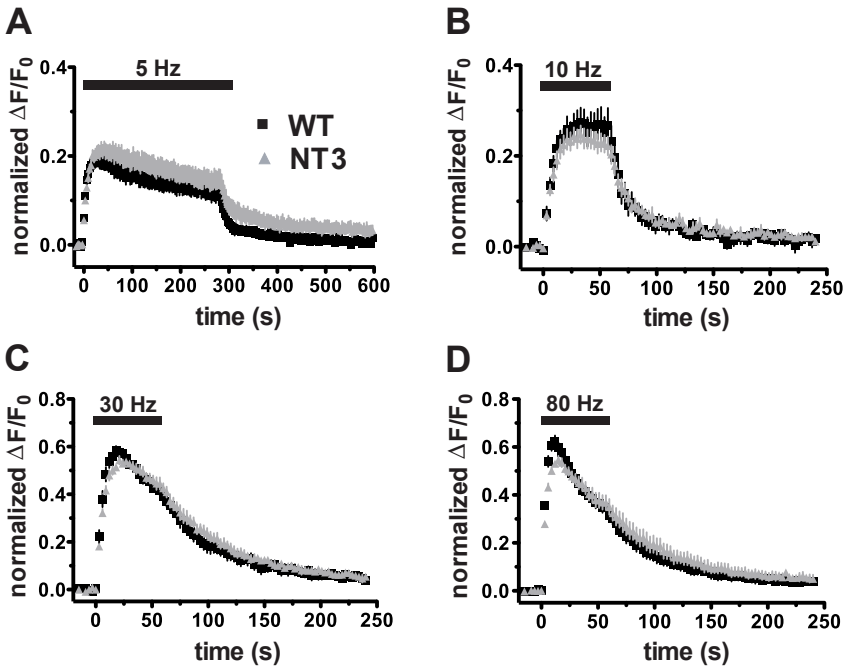

Figure 5

Figure 5: Mutation of the N-terminal dileucine-like motifs does not significantly impair endocytosis.

Time course of fluorescence changes in neurons transfected with WT VGLUT1-pH (black) or NT3 VGLUT1-pH (grey) with 5 Hz for 5 min (**A**), 10 Hz for 1 min (**B**), 30 Hz for 1 min (**C**) or 80 Hz for 1 min (**D**) stimulation (black bars). Each trace was normalized to the size of the total pool of VGLUT1-pH as determined by application of modified Tyrode's solution containing 50 mM NH_4Cl. No differences are observed with the NT3 mutation relative to WT. All data mean ± SEM of n = 5-20 coverslips from at least 2 independent cultures with > 20 synapses analyzed per coverslips.

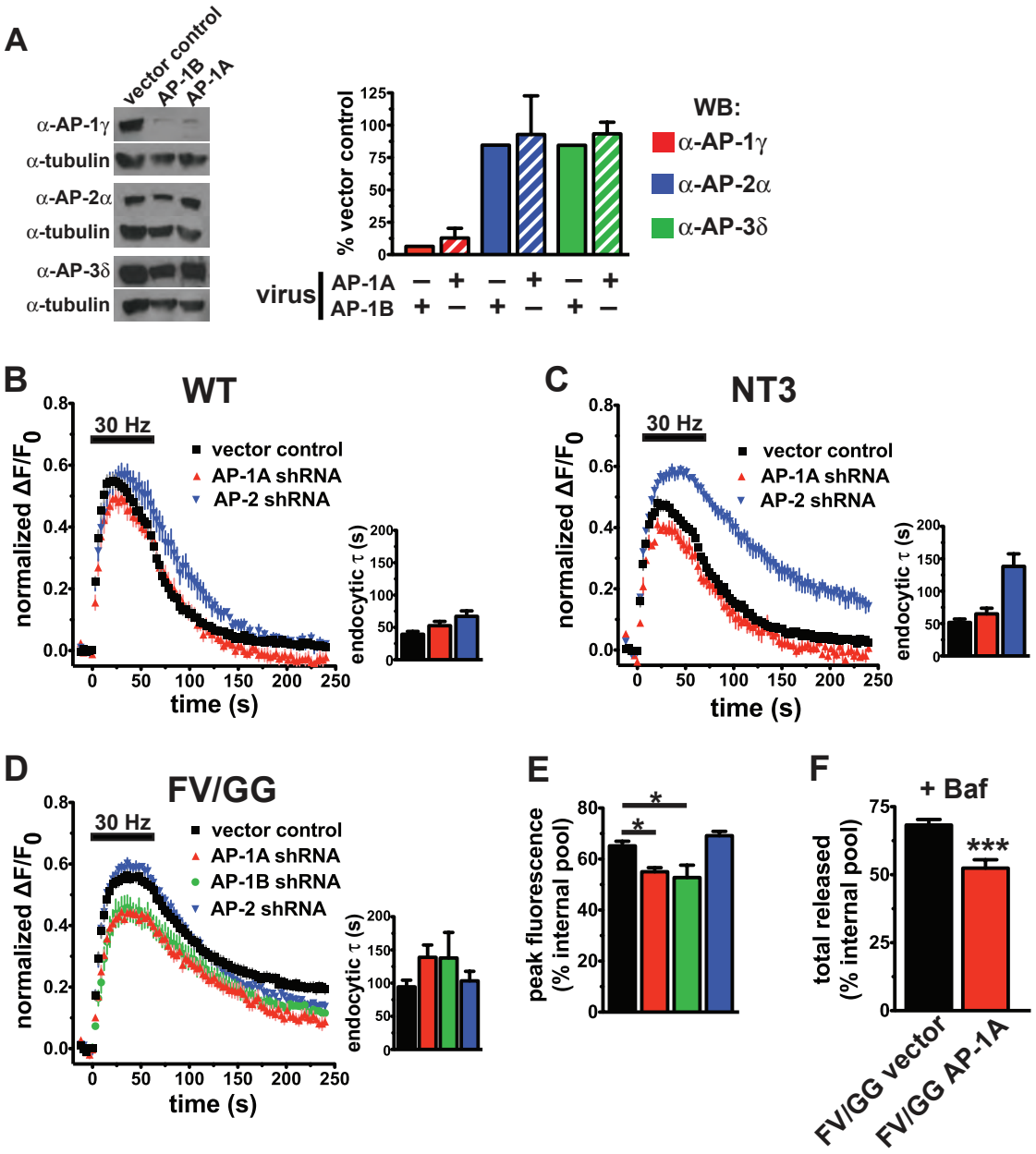
A
vector control
AP-1B
AP-1A
α-AP-1γ
α-tubulin
α-AP-2α
α-tubulin
α-AP-3δ
α-tubulin
% vector control
WB:
α-AP-1γ
α-AP-2α
α-AP-3δ
virus
AP-1A
AP-1B
B
WT
30 Hz
vector control
AP-1A shRNA
AP-2 shRNA
normalized ΔF/F0
time (s)
endocytic τ (s)
C
NT3
30 Hz
vector control
AP-1A shRNA
AP-2 shRNA
normalized ΔF/F0
time (s)
endocytic τ (s)
D
FV/GG
30 Hz
vector control
AP-1A shRNA
AP-1B shRNA
AP-2 shRNA
normalized ΔF/F0
time (s)
endocytic τ (s)
E
peak fluorescence (% internal pool)
F
+ Baf
total released (% internal pool)
FV/GG vector
FV/GG AP-1A

Figure 6

Figure 6: N- and C-terminal dileucine-like motifs utilize different clathrin adaptor proteins.

A, Western blotting of cell lysates from primary hippocampal neurons infected with lentiviral particles containing shRNA constructs demonstrates that only AP-1 levels are reduced by the AP-1A and AP-1B hairpins. Graph: quantification of AP protein levels normalized to tubulin controls. Data shown as percentage of vector controls.

B, Time course of fluorescence changes in neurons transfected with WT VGLUT1-pH and infected with viral particles expressing empty vector (black), AP-1A shRNA (red), or AP-2 shRNA (blue), during and after stimulation at 30 Hz for 1 min (bar). Each trace was normalized to the size of the total pool of VGLUT1-pH, determined by NH_4Cl application. Knockdown of AP-2 (blue), but not AP-1 (red), significantly slows post-stimulus endocytosis of WT VGLUT1-pH. (vector control: τ_{decay} = 39.5 ± 4.2 s; AP-1A: τ_{decay} = 52.6 ± 6.6 s; AP-2: τ_{decay}= 67.1 ± 8.5 s) (compared to vector control: AP-2, $p < 0.05$; AP-1A, $p > 0.05$; one-way ANOVA, Tukey's post-test).

C, Depletion of AP-2, but not AP-1, also significantly slows post-stimulus endocytosis of NT3 VGLUT1-pH (vector control (black): τ_{decay} = 51.7 ± 5.2 s; AP-1A (red): τ_{decay} = 64.9 ± 8.8 s; AP-2 (blue): τ_{decay} = 138.2 ± 19.4 s) (compared to vector control: AP-2, $p < 0.001$; AP-1A, $p > 0.05$; one-way ANOVA, Tukey's post-test).

D, The rate of post-stimulus endocytosis of FV/GG VGLUT1-pH was not altered by knockdown of either AP-1 nor AP-2 (vector control (black): τ_{decay} = 94.4 ± 10.0 s; AP-1A (red): τ_{decay} = 138.9 ± 18.5 s; AP-1B (green): τ_{decay} = 137.9 ± 38.5 s; AP-2 (blue): τ_{decay} = 103.4 ± 14.3 s) ($p > 0.05$ for all comparisions; one-way ANOVA, Tukey's post-test).

E, Knockdown of AP-1, but not AP-2, lowers the peak fluorescence of FV/GG VGLUT1-pH during stimulation, normalized to the total internal pool (vector control (black): 65.2 ± 1.8%; AP-1A (red): 55.0 ± 1.6%; AP-1B (green): 52.7 ± 4.8%; AP-2 (blue): 69.2 ± 1.7%) (compared to vector control: AP-1A, $p < 0.05$, *; AP-1B, $p < 0.05$, *; AP-2, $p > 0.05$; one-way ANOVA, Tukey's post-test).

F, Stimulation in the presence of the H^+ATPase inhibitor, bafilomycin, reveals that AP-1 KD significantly decreases the fraction of the total internal pool of FV/GG VGLUT1-pH released with a 30 Hz 1 min stimulus (vector control (black): 68.3 ± 2.1%; AP-1A (red): 52.4 ± 3.1%) ($p = 0.0006$, ***, unpaired, two-tailed t-test).

All data shown as mean ± SEM. For B-F, n = 5-20 coverslips from at least 2 independent cultures with > 20 synapses analyzed per coverslip.

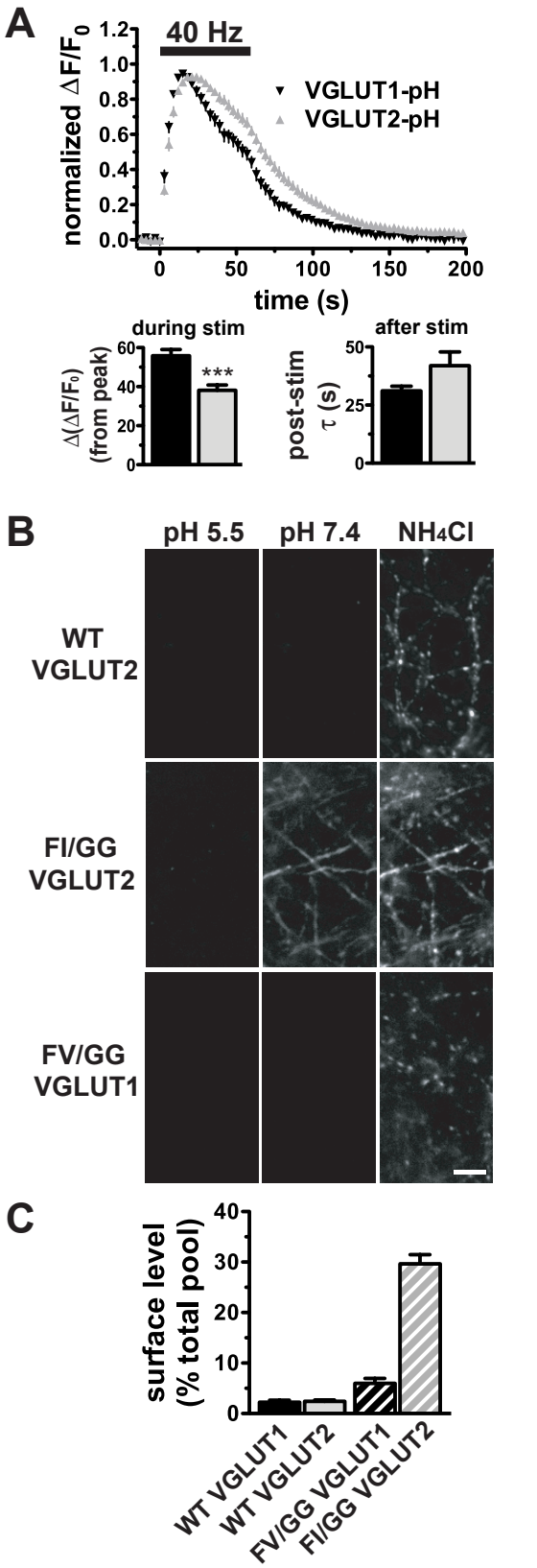
A
40 Hz
normalized ΔF/F0
VGLUT1-pH
VGLUT2-pH
time (s)
during stim
after stim
Δ(ΔF/F0) (from peak)
post-stim τ (s)
***
B
pH 5.5
pH 7.4
NH4Cl
WT VGLUT2
FI/GG VGLUT2
FV/GG VGLUT1
C
surface level (% total pool)
WT VGLUT1
WT VGLUT2
FV/GG VGLUT1
FI/GG VGLUT2

Figure 7

Figure 7: VGLUT1 and VGLUT2 differ in their trafficking.

A, Time course of fluorescence changes in neurons transfected with either WT VGLUT1-pH (black) or VGLUT2-pH (grey) to a 40 Hz for 1 min stimulation (bar). Traces normalized to peak fluorescence during stimulation. The extent of fluorescence decay [$\Delta(\Delta F/F_0)$] during stimulation is greater for VGLUT1 than VGLUT2 (VGLUT1: 55.8 ± 3.2% of peak F; VGLUT2: 38.2 ± 2.6% of peak F; $p < 0.0006$, ***, unpaired, two-tailed t-test) (bottom left inset). The rate of VGLUT2 post-stimulus endocytosis is not significantly slower than VGLUT1 (VGLUT1 τ_{decay} = 31.2 ± 1.9 s, VGLUT2: τ_{decay} = 41.9 ± 5.9 s, $p = 0.12$, unpaired, two-tailed t-test) (bottom right inset). For all graphs, n = 8–9 coverslips from 4 independent cultures with > 20 synapses analyzed per coverslip.

B, Hippocampal neurons transfected with WT VGLUT2-pH, FI/GG VGLUT2-pH, or FV/GG VGLUT1-pH were imaged in Tyrode's solution buffered with MES to pH 5.5 to quench surface fluorescence, at rest (pH 7.4), and upon alkalinization in NH_4Cl to measure total fluorescence. Significant fluorescence is observed with FI/GG VGLUT2-pH at rest (pH 7.4) that is quenched by pH 5.5 Tyrode's solution, indicating that a large amount of the transporter is present on the cell surface at rest.

C, At rest, the cell surface expression of WT VGLUT1-pH (2.2 ± 0.4% of total protein) and WT VGLUT2-pH (2.4 ± 0.3% of total protein) are similar ($p = 0.65$, unpaired, two-tailed t-test). In contrast, considerably more FI/GG VGLUT2-pH is on the cell surface at rest than FV/GG VGLUT1-pH (FV/GG: 6.0 ± 1.0%, FI/GG: 29.7 ± 1.8%, $p < 0.0001$, unpaired, two-tailed t-test). n = 5-15 coverslips from at least 4 independent cultures with > 20 synapses analyzed per coverslip. Data for WT and FV/GG VGLUT1-pH from Fig. 1C.

Data are mean ± SEM.

Chapter 3:

Protein Interactions with the C-terminus of VGLUT1.

Introduction

Examination of the C-terminus of VGLUT1 reveals two polyproline motifs: PP1 and PP2. Since these polyproline motifs are not found in the other VGLUT isoforms, their presence could help explain some of the functional differences observed between the transporters. Polyproline motifs can contain consensus binding sites for SH3 domains (PxxP) and/or WW domains (PPxY) (T. Pawson, 1995; M. J. Macias et al., 2002). SH3 and WW domains are protein interactions moieties found in a wide-range of cellular proteins. A previous yeast two hybrid screen identified endophilin I, II, and III as VGLUT1 interactors. Further work confirmed that that the endophilins bind to the more distal motif, PP2 (S. M. Voglmaier et al., 2006). This interaction was also independently identified by two other research groups (S. De Gois et al., 2006; J. Vinatier et al., 2006).

The interaction between PP2 and endophilin directs VGLUT1 towards a fast, AP-2 dependent endocytic pathway, away from a slower AP-1/3 dependent pathway (S. M. Voglmaier et al., 2006). Recent work has demonstrated that the differences in glutamate release mediated by VGLUT1 and -2 are due to this interaction with endophilin, although the mechanism remains unclear (M. C. Weston et al., 2011).

Given the importance of the endophilin interaction with PP2 on VGLUT1 function, I searched for potential interactors with the other polyproline motif, PP1.

Materials and Methods

Molecular biology

His-PP1 was generated by inserting the PP1 sequence into the ligand expression vector provided with the TransSignal WW and SH3 domain arrays (Panomics). Myc-tagged Lyn was generated by amplifying full-length mouse Lyn (kind gift of C. Abram, Lowell lab, UCSF) with a myc tag followed by a four alanine linker immediately before the kinase. The resulting Myc-Lyn was subcloned into the pcDNA1/Amp (Invitrogen) vector using standard techniques. GST fusions of the C-terminus of VGLUT1 with various mutations were generated by amplification of the C-terminal fragments via PCR and subsequent subcloning into the pGEX-3X vector (GE Lifesciences). GST fusions of the SH3 domains of human Fyn and Src in pGEX vectors along with full-length mouse Lyn were kind gifts of C. Abram (Lowell lab, UCSF). Purified GST-Lyn-SH3 protein was purchased from Panomics. Full-length WT and dominant negative Nedd4.1 and AIP4 fused to mCherry (kind gift of M. von Zastrow, UCSF) were subcloned into the pCAGGS vector using standard techniques.

SH3 and WW domain array

Bacterial cultures expressing His-PP1 by IPTG induction were lysed according to the manufacturer's instructions for the TransSignal domain arrays. The resulting lysate was then incubated with the array blots and His-PP1 was detected according to manufacturer's instructions.

GST pulldowns

GST fusion proteins were expressed in XL1-Blue bacteria via induction with 0.5 mM IPTG. Bacterial pellets were resuspended in PBS-CMF containing bacterial protease inhibitors (Sigma) and lysed via sonication. Centrifugation-cleared supernatants were

incubated with glutathione beads and protein concentration determined using the Bradford assay. Protein concentrations were then normalized by the addition of unbound glutathione beads. Glutathione bead-bound GST proteins were then incubated with either COS7 lysates or rat brain extracts. After multiple washes, bound proteins were eluted from the beads using 1X SDS sample buffer and boiling for 5 min (when appropriate). Proteins were separated using gel electrophoresis and detected with Western blotting using appropriate antibodies. COS7 cells were transfected with myc-Lyn by electroporation (Bio-Rad Gene Pulser II).

Results

As previously mentioned, the C-terminus of VGLUT1 contains two polyproline motifs that are not found in VGLUT2 or -3. The more distal motif, PP2, interacts with the endocytic protein endophilin (S. De Gois et al., 2006; J. Vinatier et al., 2006; S. M. Voglmaier et al., 2006). However, no interactor has been identified for the more proximal motif, PP1. Since PP1 contains consensus binding sites for both SH3 (PxxP) and WW (PPxY) domains, I used TransSignal SH3 domain arrays I-IV and WW domain arrays I-II (Panomics) to screen for potential PP1 interactors. The domain arrays consisted of purified GST fusions of SH3 or WW domains from a wide-range of cellular protein spotted, in duplicate, onto a membrane suitable for Western blotting. The arrays cover the majority of identified SH3 and WW domains found in the human genome. To detect potential PP1 interactors, the arrays were incubated with bacterial lysates containing His-PP1. Binding of his-tagged peptide to proteins on the membrane was

detected using anti-his antibodies. Numerous potential interactors were identified and are listed in Fig. 2 and 3, next to pictures of the appropriate domain array. Notable SH3 domain proteins included multiple Src family tyrosine kinases (Fyn, Lyn, Src, Hck), scaffolding/adaptor proteins (Nck1, Nck2, intersectin, ArgBP2, sorting nexin 9), proteins with unknown functions (OSF), and endophilin (Fig. 2). Notable WW domain proteins included multiple E3 ubiquitin ligases (Nedd4, AIP4, WWP1, WWP2) (Fig. 3).

To confirm these putative interactors, I performed GST pulldowns using GST fusions of the C-terminus of VGLUT1 with various mutations and deletions. I then detected binding of the candidate interactors using Western blotting with appropriate antibodies. Using this approach, I found that the scaffolding protein CAP/ponsin, which is involved in cytoskeletal regulation and cell signaling (N. Kioka et al., 2002), specifically binds PP2 (Fig. 4A). Another scaffolding protein, Nck1/2, also binds specifically to PP2 (L. Buday et al., 2002) (Fig. 4A). PP2 also appears to be the interaction site for the Src-family tyrosine kinase, Lyn (Fig. 4B). The SH3 domain of Lyn also binds VGLUT1 to much greater extent than the SH3 domains of the other Src-family kinases, Src and Fyn (Fig. 4C).

One protein that did interact with PP1 was the WW domain containing E3 ligase AIP4 (alternatively known as Itch) (G. Melino et al., 2008) (Fig. 4A). Consistent with the fact that AIP4 contains four WW domains, it appears to specifically interact with the WW domain consensus binding site, PPxY, at the end of PP1. This is demonstrated by the fact that the PAXA and PAXY mutants that disrupt this site also disrupt AIP4 binding while elimination of the three SH3 domain consensus binding sites by the PXXP123 mutant does not affect AIP4 binding.

To determine if AIP4 regulates VGLUT1 recycling, I co-transfected dominant negative full-length AIP4 (AIP4 C/A) with FV/GG VGLUT1-pH. Other work (see Chapter 4) had demonstrated that mutation of the PPxY motif improves the endocytosis of FV/GG VGLUT1. I hypothesized that if AIP4 is responsible for this effect via its interaction with PPxY, expression of a dominant negative AIP4 construct should replicate the effect of the PAXA mutation. Since certain GST pulldown experiments suggested that Nedd4 may also bind VGLUT1, although the results were rarely clear, I also did co-transfections with either WT or dominant negative full-length Nedd4.1. To maximize expression of the AIP4 and Nedd4 constructs, neurons were transfected with 0.5 μg of FV/GG VGLUT1-pH DNA and 4.5 μg of AIP4/Nedd4 DNA. Surprisingly, both WT and dominant negative (C/A) Nedd4.1 improved FV/GG VGLUT1-pH endocytosis but not dominant negative AIP4 (Fig. 5). While only one experiment was completed due to time constraints, this preliminary result suggests that Nedd4, and not AIP4, regulates VGLUT1 recycling.

Discussion

While screening for proteins that interact with PP1, I identified three additional proteins that interact with PP2 *in vitro*: Nck1/2, CAP/ponsin, and Lyn. The role that these interactors might play in VGLUT1 function is unclear. Lyn, a Src-family tyrosine kinase, would presumably phosphorylate tyrosine residues in VGLUT1 or other proteins that interact with the transporter. A related kinase, Fyn, has been shown to phosphorylate AIP4 and disrupt its interaction with a protein that it ubiquinates (C. Yang et al., 2006).

Another related kinase, Src, has been reported to phosphorylate endophilin A2 (X. Wu et al., 2005). Nck1 and -2 are implicated in the remodeling of the actin cytoskeleton and also interact with numerous signaling molecules (L. Buday et al., 2002). CAP/ponsin, like Nck1/2, has also been implicated in regulation of the actin cytoskeleton and various cell signaling pathways so the function that it could serve in VGLUT1 function is not readily apparent (N. Kioka et al., 2002).

Nedd4 and/or AIP4 would presumably regulate VGLUT1 function by ubiquinating the transporter itself or another protein in close proximity, possibly one that also binds VGLUT1. AIP4 has been shown to ubiquinate both endophilin and Lyn (G. Winberg et al., 2000; A. Angers et al., 2004). VGLUT1 also contains two lysine residues, Lys-494 and Lys-507, within a putative PEST domain that could potentially be ubiquinated. Intriguingly, while mutation of these residues OR the dileucine portion of the C-terminal dileucine-like motif (FV/GG) alone does not disrupt expression of the transporter, initial experiments suggest that combining these mutants prevents either expression of the transporter or its trafficking out of the biosynthetic pathway (data not shown). While these results are interesting, much work remains to be done to confirm that Nedd4 actually regulates VGLUT1 trafficking.

References

Angers A, Ramjaun AR, McPherson PS (2004) The HECT domain ligase itch ubiquitinates endophilin and localizes to the trans-Golgi network and endosomal system. J Biol Chem 279:11471-11479.

Buday L, Wunderlich L, Tamas P (2002) The Nck family of adapter proteins: regulators of actin cytoskeleton. Cell Signal 14:723-731.

De Gois S, Jeanclos E, Morris M, Grewal S, Varoqui H, Erickson JD (2006) Identification of endophilins 1 and 3 as selective binding partners for VGLUT1 and their co-localization in neocortical glutamatergic synapses: implications for vesicular glutamate transporter trafficking and excitatory vesicle formation. Cell Mol Neurobiol 26:679-693.

Kioka N, Ueda K, Amachi T (2002) Vinexin, CAP/ponsin, ArgBP2: a novel adaptor protein family regulating cytoskeletal organization and signal transduction. Cell Struct Funct 27:1-7.

Macias MJ, Wiesner S, Sudol M (2002) WW and SH3 domains, two different scaffolds to recognize proline-rich ligands. FEBS Lett 513:30-37.

Melino G, Gallagher E, Aqeilan RI, Knight R, Peschiaroli A, Rossi M, Scialpi F, Malatesta M, Zocchi L, Browne G, Ciechanover A, Bernassola F (2008) Itch: a HECT-type E3 ligase regulating immunity, skin and cancer. Cell Death Differ 15:1103-1112.

Pawson T (1995) Protein modules and signalling networks. Nature 373:573-580.

Vinatier J, Herzog E, Plamont MA, Wojcik SM, Schmidt A, Brose N, Daviet L, El Mestikawy S, Giros B (2006) Interaction between the vesicular glutamate transporter type 1 and endophilin A1, a protein essential for endocytosis. J Neurochem 97:1111-1125.

Voglmaier SM, Kam K, Yang H, Fortin DL, Hua Z, Nicoll RA, Edwards RH (2006) Distinct endocytic pathways control the rate and extent of synaptic vesicle protein recycling. Neuron 51:71-84.

Weston MC, Nehring RB, Wojcik SM, Rosenmund C (2011) Interplay between VGLUT isoforms and endophilin A1 regulates neurotransmitter release and short-term plasticity. Neuron 69:1147-1159.

Winberg G, Matskova L, Chen F, Plant P, Rotin D, Gish G, Ingham R, Ernberg I, Pawson T (2000) Latent membrane protein 2A of Epstein-Barr virus binds WW domain E3 protein-ubiquitin ligases that ubiquitinate B-cell tyrosine kinases. Mol Cell Biol 20:8526-8535.

Wu X, Gan B, Yoo Y, Guan JL (2005) FAK-mediated src phosphorylation of endophilin A2 inhibits endocytosis of MT1-MMP and promotes ECM degradation. Dev Cell 9:185-196.

Yang C, Zhou W, Jeon MS, Demydenko D, Harada Y, Zhou H, Liu YC (2006) Negative regulation of the E3 ubiquitin ligase itch via Fyn-mediated tyrosine phosphorylation. Mol Cell 21:135-141.

A

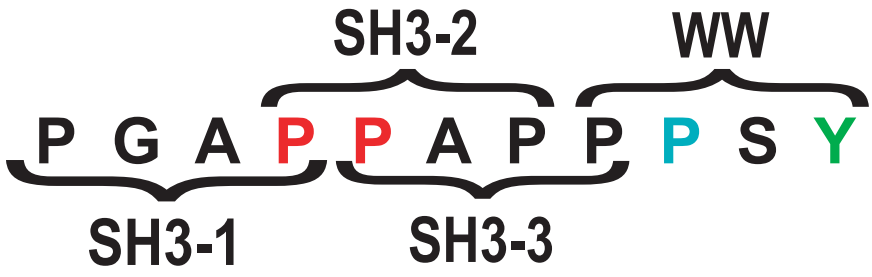

B

```
      WT: PPGAPPAPPPSYGATHSTVQPPRPPPP
   ΔPP1: ----------**********
   ΔPP2: **********----------
   PAXA: ********A**A**********
   PAXY: ********A**********
PxxP123: ****AA**********
```

Figure 1

Figure 1: Diagram of the first polyproline motif (PP1) of VGLUT1.

A, The first polyproline motif (PP1) of VGLUT1 contains 3 consensus binding sites for an SH3 domain (PxxP, SH3 I-III) and 1 consensus binding site for a WW domain (PPxY, WW). All three SH3 domain consensus binding sites were disrupted by mutation of Pro-544 and Pro-545, highlighted in red, to alanine in order to generate the PxxP123 mutant. The WW domain consensus binding site was disrupted by mutation of Pro-539 (teal) to alanine with or without mutation of Tyr-541 (green) to generate either the PAXA or PAXY mutants.

B, Diagram of mutants used in *in vitro* binding experiments. Unaltered residues are indicated by '*' and deleted residues are indicated by '-'.

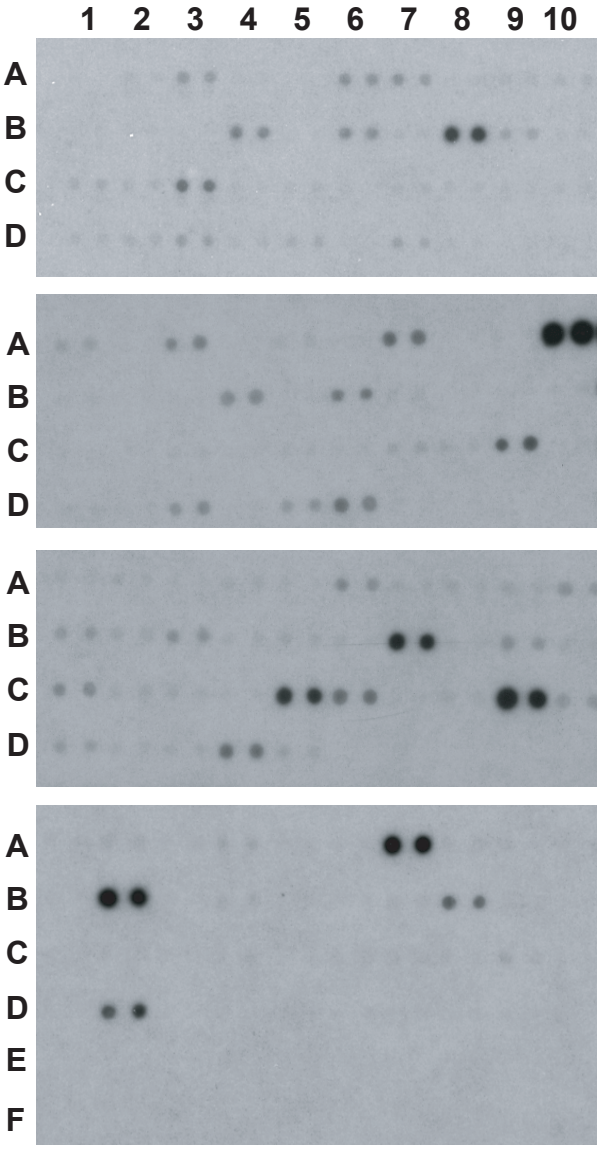

SH3 I:

3A: Spectrin a-chain
3C: ARHGEF 7
4B: Fyn
6A: Yes1
6B: Src
7A:Abl2
8B: Hck

SH3 II:

1A: Abl1 I2
3A: Abl2
3D: VAV-3
4B: Tec
9C: SNX9
5D: Vinexin
6B: PLCγ2
6D: Src
7A: Nck1-D3
10A: OSF

SH3 III:

4D: Src
5C: Nck2-D1
6C: NPH1
7B: Lyn
9C: endophilin A1

SH3 IV:

2B: Nck1-D1
2D: EPS8
7A: ArgBP2-D2
8B: Intersectin

Figure 2

Figure 2: Screen for SH3 domains that interact with PP1 motif of VGLUT1.

SH3 domain arrays, consisting of purified GST-fusions of SH3 domains from various proteins spotted in duplicate, were incubated with bacterial lysate containing his-tagged PP1 peptide. Binding of his-PP1 peptide was detected using anti-his antibodies. Listed are the putative interactors detected on each array.

Table 1: List of Domains Present on SH3 Domain Array I

Position	Domain	Full Name
A1	Amphiphysin	Amphiphysin
B1	Dlg2	Discs large homolog 2
C1	VAV-D1	VAV proto-oncogene, SH3 domain #1
D1	BLK	Beta-lymphocyte specific protein tyrosine kinase
A2	LCK	Human T-lymphocyte specific protein tyrosine kinase p56 LCK
B2	EMP55	55 kDa erythrocyte membrane protein
C2	NCK1-D3	Cytoplasmic protein NCK1, SH3 domain #3
D2	Abl	Abelson tyrosine kinase
A3	SPCN	Spectrin alpha chain (non-erythrocytic)
B3	FGR	Cellular Gardner-Rasheed feline sarcoma virus protein
C3	Y124	PAK-interacting exchange factor beta
D3	PLCγ	Phospholipase C gamma-1
A4	Cortactin	Cortactin
B4	SLK	Proto-oncogene tyrosine protein kinase FYN
C4	PEXD	Peroxisomal membrane protein PEX13
D4	Riz	Retinoblastoma protein-interacting zinc-finger
A5	MLPK3	Mixed-lineage kinase 3
B5	Nebulin	Nebulin
C5	BTK	Bruton Tyrosine Kinase
D5	PI3b	Phosphoinositide-3-kinase regulatory beta subunit
A6	Yes1	Yamaguchi sarcoma virus oncogene homolog 1
B6	c-Src	Cellular Rous Sarcoma viral oncogene homolog
C6	RasGAP	Ras GTPase-activating protein 1
D6	ITSN-D1	Intersectin, SH3 Domain #1
A7	Abl2	Abelson-related protein; Arg
B7	FYB-D1	Fyn binding protein, SH3 domain #1
C7	PSD95	Presynaptic density protein 95
D7	ITSN-D2	Intersectin, SH3 Domain #2
A8	SJHUA	Spectrin alpha chain, erythrocyte
B8	Hck	Hemopoietic cell kinase
C8	Tim	Rho guanine nucleotide exchange factor (GEF) 5
D8	TXK	Tyrosine-protein kinase TXK
A9	Itk	Interleukin-2-inducible T-cell kinase
B9	VAV2-D2	Vav2 oncogene product, SH3 Domain #2
C9	HS1	Hematopoietic specific protein 1
D9	GST	Glutathione-S-transferase
A10	CRK-D2	Avian sarcoma virus CT10 oncogene homolog, domain #2
B10	NOF2-D1	Neurite outgrowth factor or neutrophil cytosol factor 2, domain #1
C10	Stam	Signal transducing adaptor molecule

Table 2: List of Domains Present on SH3 Domain Array II

Position	Domain	Full Name
A1	Abl2B	Abl interactor protein 2
B1	PI3a	Phosphatidylinositol 3-kinase regulatory alpha subunit
C1	GRAP-D1	GRB2-related adaptor protein, SH3 Domain #1
D1	VAV2-D1	Vav-2 protein, SH3 Domain #1
A2	GRB2L-D1	Grb2-related adaptor protein 2, SH3 Domain #1
B2	SP93	Channel associated protein of synapse-110
C2	JIP1	C-jun-amino-terminal kinase interacting protein 1
D2	VAV3-D1	Vav-3 protein, SH3 Domain #1
A3	Abl2	Abelson-related protein; Arg
B3	STAC	Stac protein
C3	M3KA	Mitogen-activated protein kinase kinase kinase 10
D3	VAV3-D2	Vav-3 protein, SH3 Domain #2
A4	CCBA	Dihydropyridine-sensitive L-type, calcium channel beta-1 subunit
B4	Tec	Tyrosine-protein kinase Tec
C4	MY7A	Myosin VIIa
D4	VINE-D1	Vinexin, SH3 Domain #1
A5	CRKL-D1	CRK-like protein, SH3 Domain #1
B5	TRIP10	Cdc42-interacting protein 4
C5	NCK2-D2	Cytoplasmic protein NCK2, SH3 Domain #2
D5	VINE-D3	Vinexin, SH3 Domain #3
A6	CSKP	Peripheral plasma membrane protein CASK
B6	PIG2	1-phosphatidylinositol-4,5-biphosphate phosphodiesterase gamma2
C6	NCK2-D3	Cytoplasmic protein NCK2, SH3 Domain #3
D6	c-Src	Cellular Rous Sarcoma viral oncogene homolog
A7	NCK1-D2	Cytoplasmic protein NCK1, SH3 Domain #2
B7	ARH6	Rho guanine nucleotide exchange factor 6
C7	RHG4	Rho-GTPase-activating protein 4
D7	GST	negative control
A8	NE-DLG	Presynaptic protein SAP102
B8	BCA1	CRK-associated substrate
C8	SH31	SH3-containing GRB2-like protein 1
D8	empty	
A9	NOF2-D2	Neutrophil cytosol factor 2, SH3 Domain #2
B9	BIN1	Myc box dependent interacting protein 1
C9	SNX9	Sorting nexin 9
D9	empty	
A10	OSF	Osteoclast stimulating factor 1
B10	EFS	Embryonal Fyn-associated substrate
C10	UAS3	UBASH3A

Table 3: List of Domains Present on SH3 Domain Array III

Position	Domain	Full Name
A1	PRMT2	Arginine N-methyltransferase 2
B1	Grb2-D1	Growth factor receptor-bound protein 2, SH3 Domain #1
C1	MY1E	Myosin-IE
D1	SPIN90	SH3 Protein Interacting with Nck, 90 kDa
A2	BMX	Grb2-related adaptor protein 2, SH3 Domain #1
B2	Grb2-D2	Growth factor receptor-bound protein 2, SH3 Domain #2
C2	MY1F	Myosin-IF
D2	Trio	Triple functional domain protein
A3	BPAG1	Bullous pemphigoid antigen
B3	Grap-2-D2	Grb-2 related adaptor protein 2, SH3 Domain #2
C3	NCF1-D1	47 kDa neutrophil oxidase factor (p47-phox), SH3 Domain #1
D3	VINE-D2	Vinexin, SH3 Domain #2
A4	CACNB2	Voltage-dependent calcium channel beta-2-subunit
B4	ITSN-D3	Intersectin 1, SH3 Domain #3
C4	NCF1-D2	47 kDa neutrophil oxidase factor (p47-phox), SH3 Domain #2
D4	c-SRC	Cellular Rous Sarcoma viral oncogene homolog
A5	CRK-D1	Proto-oncogene CRK, SH3 Domain #1
B5	ITSN-D4	Intersectin 1, SH3 Domain #4
C5	Nck2-D1	Cytoplasmic protein NCK2, SH3 Domain #1
D5	GST	Glutathione-S-Transferase
A6	CRK-D2	Proto-oncogene CRK, SH3 Domain #2
B6	JIP2	C-jun-amino-terminal kinase interacting protein 2
C6	NPH1	Juvenile nephronophthisis 1 protein
D6	Empty	
A7	CRKL-D2	Crk-like protein, SH3 Domain #2
B7	Lyn	lck/yes-related novel (LYN) protein tyrosin kinase
C7	OTOR	Otoraplin
D7	Empty	
A8	FYB-D2	FYN-binding protein, SH3 Domain #2
B8	ZO2	Zonula occludens 2 protein
C8	Dlg1	Synapse-associated protein 97 (SAP97)
D8	Empty	
A9	GAP	GTPase-activating protein
B9	MATK	Megakaryocyte-associated tyrosine-protein kinase
C9	SH3GL2	SH3-containing GRB2-like protein 2
D9	Empty	
A10	Grap-D2	Grb2-related adaptor protein, SH3 Domain #2
B10	MIA	Melanoma inhibitory activity
C10	SH3GL3	SH3-containing GRB2-like protein 3

Table 4: List of Domains Present on SH3 Domain Array IV

Position	Accession #	Domain	Full Name
A1	NP_062541	ITSN(2)-D1	Intersectin 2, Domain #1
A2	NP_062541	ITSN(2)-D2	Intersectin 2, Domain #2
A3	NP_062541	ITSN(2)-D3	Intersectin 2, Domain #3
A4	NP_054782	HIP-55	src homology 3 domain-containing protein HIP-55
A5	NP_009160	PACSIN2	protein kinase C and casein kinase in neurons 2; pacsin 2
A6	NP_006139	LASP1	LIM and SH3 protein 1, Lasp-1
A7	NP_003594	ARGBP2-D2	Arg/Abl-interacting protein 2, Domain #2
A8	NP_003594	ARGBP2-D3	Arg/Abl-interacting protein 2, Domain #3
A9	NP_005834	STAM2	STAM-like protein containing SH3 and ITAM 2
A10	AAK37563	SORBS-D3	sorbin and SH3 domain containing 1, Domain #3
B1	NP_003015	ITSN(1)-D4	Intersectin 1, Domain #4
B2	NP_006144	NCK1-D1	Cytoplasmic protein NCK1, Domain #1
B3	O60301	KIAA0554	KIAA0554 protein
B4	NP_006384	NEBL	nebulette
B5	NP_004374	CSK	c-src tyrosine kinase; CSK
B6	NP_006739	SLA	Src-like adaptor; SLAP
B7	NP_005419	VAV-D2	VAV 1 proto-oncogene, Domain #2
B8	NP_003594	ARGBP2-D1	Arg/Abl-interacting protein 2, Domain #1
B9	NP_055665	SRGAP2	SLIT-ROBO Rho GTPase-activating protein 3; WAVE-associated Rac GTPase activating protein
B10	BAA32301	KIAA0456	KIAA0456 protein
C1	NP_004749	BZRAP1-D1	Peripheral benzodiazepine receptor-associated protein 1; Domain #1
C2	NP_055886	GRAF	GTPase regulator associated with the focal adhesion kinase pp125; Oligophrenin-1 like protein
C3	NP_061863	CXorf9-D1	Likely ortholog of mouse SH3 gene, Domain #1
C4	NP_003878	DDEF2	development- and differentiation-enhancing factor 2; PYK2 terminus-associated protein
C5	NP_055446	KIAA0418-D3	KIAA0418 gene product; likely ortholog of five SH3 domains; Domain #3
C6	NP_055446	KIAA0418-D4	KIAA0418 gene product; likely ortholog of five SH3 domains; Domain #4
C7	NP_055446	KIAA0418-D5	KIAA0418 gene product; likely ortholog of five SH3 domains; Domain #5
C8	NP_056000	ARHGEF9	Cdc42 guanine exchange factor 9; hPEM-2 collybistin
C9	NP_003969	PSTPIP1	Proline-serine-threonine phosphatase interacting protein 1; CD2 tail-binding protein
C10	NP_000622	NCF4	Neutrophil cytosolic factor 4 (40kD), isoform p40phox; Neutrophil cytosolic factor-4
D1	NP_006394	NEDD9	Enhancer of filamentation 1 (cas-like docking; substrate related)
D2	NP_004438	EPS8	Epidermal growth factor receptor pathway substrate

D3	NP_055263	ARHGEF16	Rho guanine exchange factor 16, GEF16
D4	NP_055639	KIAA0769-D1	KIAA0769 gene product; SH3 Domain #1
D5	NP_006331	BAIAP2	BAI1-associated protein 2, isoform 3
D6	BAA34510	KIAA0790	KIAA0790 protein
D7	NP_056131	PPP1R13B	Protein phosphatase 1, regulatory (inhibitor) subunit 13B; apoptosis-stimulating protein of p53, 1
D8	XP_098238	DKFZp434D0215-D3	similar to hypothetical protein; Domain #3
D9	XP_098238	DKFZp434D0215-D4	similar to hypothetical protein; Domain #4
D10	NP_057307	PACSIN3	protein kinase C and casein kinase in neurons 3; SH3 domain-containing protein; PACSIN3
E1	BAA86453	KIAA1139	KIAA1139 protein
E2	BAA86563	KIAA1249	KIAA1249 protein
E3	NP_056410	DKFZP434D146	DKFZP434D146 protein
E4	NP_009049	TRIO(2)	Triple functional domain (PTPRF interacting): trio protein variant 2
E5		SH3-positive control	SH3 Domain positive control for Class Ib SH3 ligand
E6		GST	Glutathione-S-Transferase

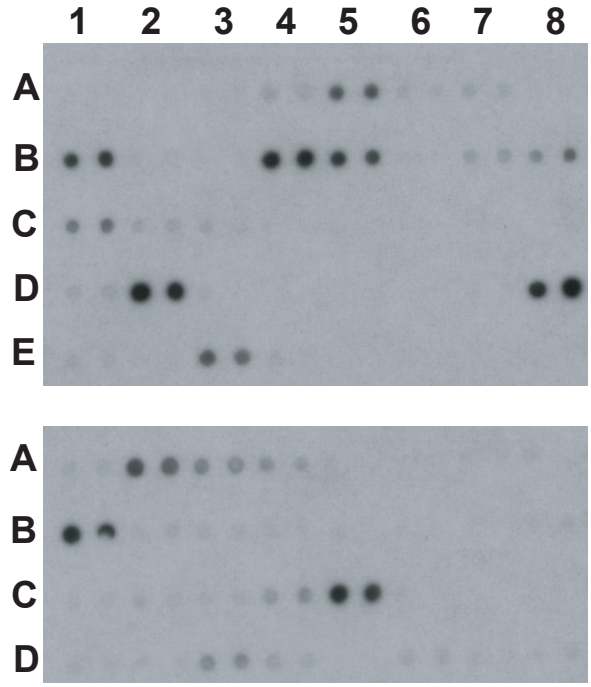

WW I:

1B: WWP2
1C: Nedd4L-D3
2D: YAP1
3E: FNBP4
4B: Nedd4-D2
5A: WWP1
5B: Nedd4-D3
8B: Nedd4L-D2
8D: MAGI3-D1

WW II:

1B: KFZp434M202
2A: ITCH-D1
3A: ITCH-D2
3D: TAZ
4A: ITCH-D3
4C: HYPA-D2
5C: HYPB

Figure 3

Figure 3: Screen for WW domains that interact with PP1 motif of VGLUT1.

WW domain arrays, consisting of purified GST-fusions of WW domains from various proteins spotted in duplicate, were incubated with bacterial lysate containing his-tagged PP1 peptide. Binding of his-PP1 peptide was detected using anti-his antibodies. Listed are the putative interactors detected on each array.

Table 5: List of Domains Present on WW Domain Array I

Position	Accession #	Domain	Full Name
A1	AAF08298	SMURF1-D1	E3 ubiquitin ligase SMURF1, WW Domain #1
A2	AAF08298	SMURF1-D2	E3 ubiquitin ligase SMURF1, WW Domain #2
A3	NP_073576	SMURF2-D2	E3 ubiquitin ligase SMURF2, WW Domain #2
A4	NP_073576	SMURF2-D1	E3 ubiquitin ligase SMURF2, WW Domain #1
A5	NP_008944	WWP1-D1	Nedd-4-like ubiquitin-protein ligase, WW Domain #1
A6	NP_008944	WWP1-D2	Nedd-4-like ubiquitin-protein ligase, WW Domain #2
A7	NP_008944	WWP1-D3	Nedd-4-like ubiquitin-protein ligase, WW Domain #3
A8	NP_008944	WWP1-D4	Nedd-4-like ubiquitin-protein ligase, WW Domain #4
B1	NP_008945	WWP2-D3	Nedd-4-like ubiquitin-protein ligase, WW Domain #3
B2	NP_008945	WWP2-D4	Nedd-4-like ubiquitin-protein ligase, WW Domain #4
B3	P46934	NEDD4-D1	Ubiquitin-protein ligase Nedd-4, WW Domain #1
B4	P46934	NEDD4-D2	Ubiquitin-protein ligase Nedd-4, WW Domain #2
B5	P46934	NEDD4-D3	Ubiquitin-protein ligase Nedd-4, WW Domain #3
B6	P46934	NEDD4-D4	Ubiquitin-protein ligase Nedd-4, WW Domain #4
B7	NP_056092	NEDD4L-D1	NEDD4-like ubiquitin ligase 3, WW Domain #1
B8	NP_056092	NEDD4L-D2	NEDD4-like ubiquitin ligase 3, WW Domain #2
C1	NP_056092	NEDD4L-D3	NEDD4-like ubiquitin ligase 3, WW Domain #3
C2	NP_056092	NEDD4L-D4	NEDD4-like ubiquitin ligase 3, WW Domain #4
C3	BAB13352	NEDL1-D1	NEDD4-like ubiquitin ligase 1, WW Domain #1
C4	BAB13352	NEDL1-D2	NEDD4-like ubiquitin ligase 1, WW Domain #2
C5	AAC14931	Caveolin-3	Caveolin-3
C6	BAA92539	KIAA1301	KIAA1301 protein
C7	NP_004272	BAG3	BAG-family molecular chaperone regulator-3
C8	NP_004634	PABPN1	Poly(A)-binding protein
D1	NP_005881	GAS7	Growth arrest-specific 7 isoform b
D2	NP_006097	YAP1	Yes-associated protein 1, 65 kD (YAP65)
D3	NP_071387	C20orf67	Chromosome 20 open reading frame 67
D4	NP_004733	BAIAP1-D1	Membrane associated guanylate kinase 1, WW Domain #1

D5	NP_004733	BAIAP1-D2	Membrane associated guanylate kinase 1, WW Domain #2
D6	O60828	JM26	Polyglutamine Binding Protein 1 (JM26 Protein)
D7	BAB56159	ARHGAP9	Rho-GTPase activating protein
D8	NP_690864	MAGI-3-D1	Membrane-associated guanylate kinase-related MAGI-3, WW Domain #1
E1	NP_690864	MAGI-3-D2	Membrane-associated guanylate kinase-related MAGI-3, WW Domain #2
E2	XP_113914	LOC201176	Similar to Rho-GTPase activating protein 12
E3		WW-pos	WW domain positive control
E4		GST	Glutathione-S-Transferase

Table 6: List of Domains Present on WW Domain Array II

Position	Accession #	Domain	Full Name
A1	NP_036433	AIP1-D2	atrophin-1 interacting protein 1, WW Domain #2
A2	NP_113671	ITCH-D1	atrophin-1 interacting protein 4, WW Domain #1
A3	NP_113671	ITCH-D2	atrophin-1 interacting protein 4, WW Domain #2
A4	NP_113671	ITCH-D3	atrophin-1 interacting protein 4, WW Domain #3
A5	NP_113671	ITCH-D4	atrophin-1 interacting protein 4, WW Domain #4
A6	NP_001930	DRP2	Dystrophin related protein 2
A7	NP_004000	DMD	dystrophin (muscular dystrophy and Becker types)
A8	NP_009055	UTRN	Utrophin; dystrophin-related protein (DRP1)
B1	Q8NT81	DKFZp434 M2023	Hypothetical 109.9 kDa protein; similar to: (formin binding protein 4; formin binding 30 [Mus musculus])
B2	Q9Y2L7	KIAA1014	KIAA1014 protein; similar to: (formin binding protein 4; formin binding30 [Mus musculus])
B3	Q9H4Z6	bA48B24	A novel protein containing a binding protein (FBP28) domain
B4	NP_009118	WBP4-D1	Formin binding protein 21, WW Domain #1
B5	NP_009118	WBP4-D2	Formin binding protein 21, WW Domain #2
B6	NP_001155	APBB1	Amyloid beta (A4) precursor protein-binding family member 1 (Fe65)
B7	Q92870	APBB2	Amyloid beta A4 precursor protein-binding family member 2 (Fe65-like protein)
B8	NP_006042	APBB3	FE65-like protein 2
C1	NP_036404	HYPC-D1	Huntington interacting protein HYPC, WW Domain #1
C2	NP_036404	HYPC-D2	Huntington interacting protein HYPC, WW Domain #2
C3	O75404	HYPA-D1	Huntington interacting protein HYPA/FBP11, WW Domain #1
C4	O75404	HYPA-D2	Huntington interacting protein HYPA/FBP11, WW Domain #2
C5	AAC26846	HYPB	Huntington interacting protein HYPB
C6	NP_006212	PIN1	PIN1-like protein; protein (peptidyl-prolyl cis/trans isomerase) NIMA-interacting 1
C7	NP_006213	PIN1L	PIN1-like protein; protein (peptidyl-prolyl cis/trans isomerase) NIMA-interacting 1-like
C8	NP_006624	IQGAP2	RasGTPase-activating-like protein IQGAP2
D1	NP_006697	TCERG1-D1	Transcription factor CA150, WW Domain #1
D2	NP_006697	TCERG1-D2	Transcription factor CA150, WW Domain #2
D3	NP_056287	TAZ	Transcriptional co-activator with PDZ-binding motif (TAZ)
D4	NP_057457	WWOX-D1	WW domain-containing oxidoreductase, isoform 1 (WWOX), WW Domain #1
D5	NP_057457	WWOX-D2	WW domain-containing oxidoreductase, isoform 1 (WWOX), WW Domain #2

D6	NP_060757	ARHGAP12	RhoGTPase activating protein 12
D7	NP_061885	PEPP2	Phosphoinositol 3-phosphate-binding protein-2
D8	NP_068590	SAV1-D2	WW45 protein, WW Domain #2
E1	NP_068590	SAV1-D1	WW45 protein, WW Domain #1
E2	-	WW post	WW domain positive control
E3	-	GST	Glutathione-S-Transferase

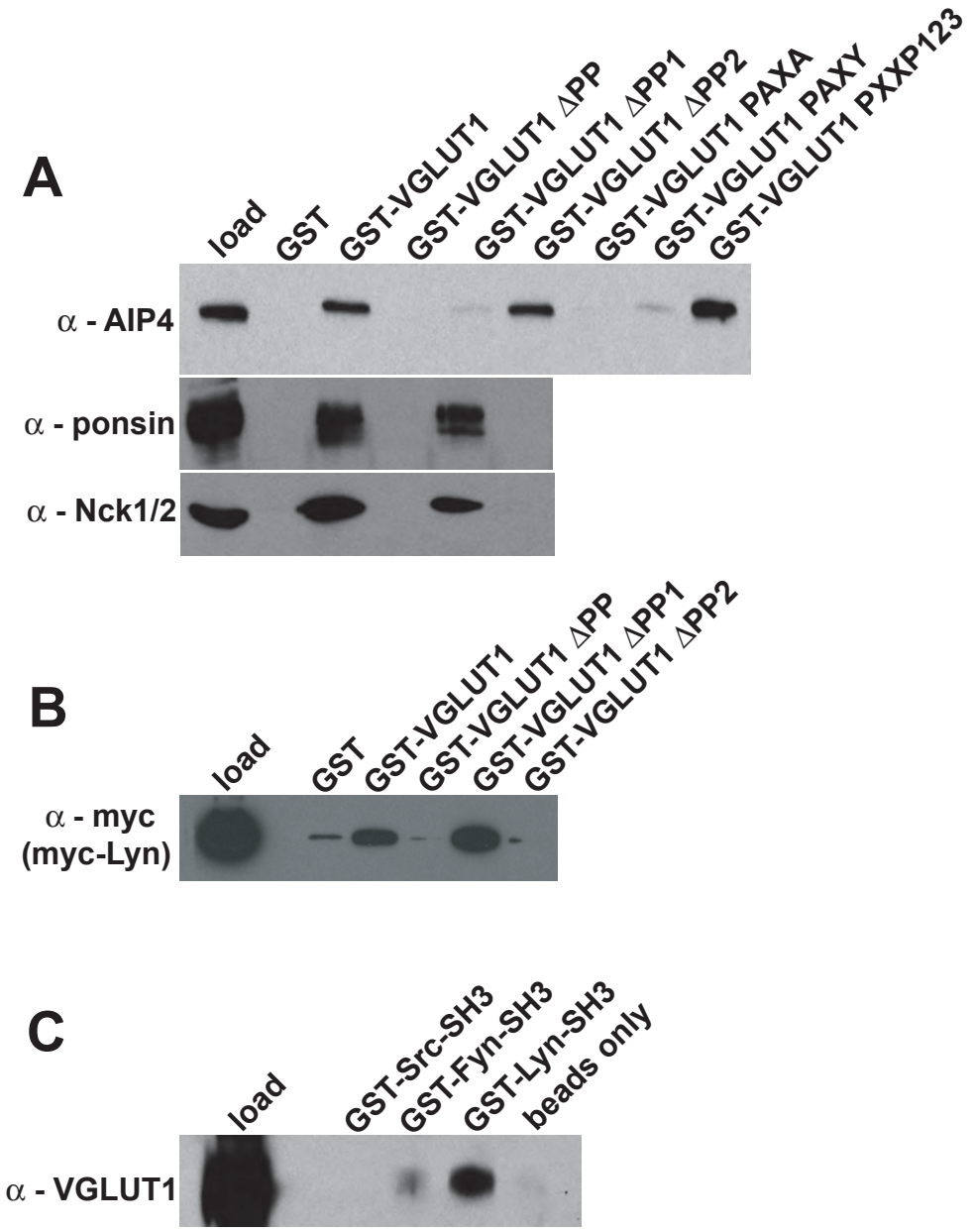
A
load
GST
GST-VGLUT1
GST-VGLUT1 ΔPP
GST-VGLUT1 ΔPP1
GST-VGLUT1 ΔPP2
GST-VGLUT1 PAXA
GST-VGLUT1 PAXY
GST-VGLUT1 PXXP123
α - AIP4
α - ponsin
α - Nck1/2
B
load
GST
GST-VGLUT1
GST-VGLUT1 ΔPP
GST-VGLUT1 ΔPP1
GST-VGLUT1 ΔPP2
α - myc
(myc-Lyn)
C
load
GST-Src-SH3
GST-Fyn-SH3
GST-Lyn-SH3
beads only
α - VGLUT1

Figure 4

Figure 4: The C-terminus of VGLUT1 interacts with multiple proteins in vitro.

A, Rat brain extract was incubated with glutathione beads bound to GST fusions of the VGLUT1 C-terminus. Bound proteins were separated by gel electrophoresis and detected by Western blotting with antibodies against AIP4, Nck1/2, or ponsin. The PPXY motif at the end of PP1 binds AIP4 while ponsin and Nck1/2 bind the second polyproline motif (PP2) of VGLUT1.

B, Lysate of COS7 cells expressing myc-Lyn was incubated with glutathione beads bound to GST fusions of the VGLUT1 C-terminus. Bound proteins were separated by gel electrophoresis and detected by Western blotting with antibodies against the myc tag. Lyn binds the PP2 motif of VGLUT1.

C, Rat brain extract was incubated with glutathione beads bound to GST fusions of the SH3 domains of the Src-family kinases Src, Fyn, and Lyn. VGLUT1 binding was detected using anti-VGLUT1 antibodies. VGLUT1 binding was strongest to the SH3 domain of Lyn.

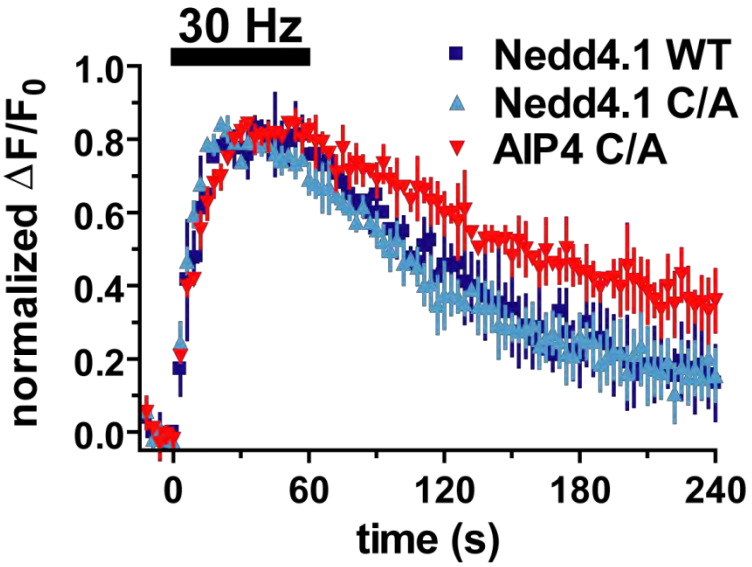
30 Hz
Nedd4.1 WT
Nedd4.1 C/A
AIP4 C/A
normalized ΔF/F0
1.0
0.8
0.6
0.4
0.2
0.0
0
60
120
180
240
time (s)

Figure 5

Figure 5: Overexpression of Nedd4.1 dominant negative alters VGLUT1 endocytosis.

Time course of pHlourin fluorescence change ($\Delta F/F_0$) in neurons transfected with FV/GG VGLUT1-pH and either Nedd4.1 WT (blue), Nedd4.1 C/A (light blue), or AIP4 C/A (red) in response to 30 Hz for 1 min stimulation (black bar). Overexpression of either WT or dominant negative Nedd4.1, but not AIP4 dominant negative, appears to improve endocytosis of FV/GG VGLUT1-pH. Traces from individual synapses were normalized to the peak fluorescence reached during stimulation and then averaged. Data are mean ± SEM of 2-4 coverslips from 1 independent culture with > 20 boutons analyzed per coverslip.

Chapter 4:

Additional Putative Trafficking Motifs in the C-terminus of VGLUT1.

Introduction

The C-terminus of VGLUT1 has been shown to contain multiple motifs that regulate its trafficking (S. De Gois et al., 2006; J. Vinatier et al., 2006; S. M. Voglmaier et al., 2006; M. C. Weston et al., 2011). In order to fully understand VGLUT1 trafficking, I further examined the C-terminal sequence for additional motifs that may serve as further sources of regulation.

Materials and Methods

Molecular biology

Various point mutations were made in the C-terminus of VGLUT1 using standard techniques. SEEK/GEEK and SEEK/DEEK VGLUT1-pH were generated by mutation of Ser-504 in VGLUT1-pH to either glycine or aspartate. SS/AA and SS/DD VGLUT1-pH were produced by mutating both Ser-519 and Ser-522 to either alanine or aspartate. FV/GG SYGAT was generated by mutation of Ser-540, Tyr-541, Gly-542, and Thr-544 to alanine in the presence of the FV/GG mutation. Various mutations were combined via standard subcloning techniques.

Results

The C-terminal dileucine-like motif that is conserved in all three VGLUT isoforms contains a serine residue immediately upstream of the two acidic glutamate residues and at the -6 position relative to the dileucine portion of the motif (Fig. 1A).

Theoretically, phosphorylation of this residue could alter the charge of the dileucine-like motif and increase affinity of this sequence to the hydrophilic patch in the recognition site found on AP proteins (B. T. Kelly et al., 2008). Comparison with the dileucine-like motifs on other transporters finds that the vesicular GABA transporter VGAT has an aspartate in this position. Recent work in our laboratory demonstrates that mutation of this residue to glycine increases the size the readily releasable pool of VGAT in a manner that is dependent on AP-3 (unpublished observations). This strongly suggests that modification of the charge at the end of a dileucine-like motif could alter AP binding. Given this finding, I tested the effect of mutation of the analogous residue in VGLUT1's C-terminal dileucine-like motif, Ser-504, to either glycine or aspartate. Initial experiments show no difference in the kinetics of VGLUT1-pH recycling, relative to WT, in response to 30 Hz stimulation for 1 min. The surface fraction of transporter at rest and the internal fluorescence at rest (representing the fraction of transporter that is internalized in non-acidified compartments) are both unaltered by either mutation.

Another potential mechanism by which VGLUT1 could be trafficked is via binding of the transporter by a member of PACS family of sorting proteins. Proteins such as PACS-1, which is the family member expressed in neurons, recognize and bind their cargo proteins via an acidic amino acid cluster containing serine and/or threonine residues that are phosphorylated by casein kinase 2 (CK2). The PACS family member in turn binds clathrin adaptor proteins such as AP-1 or -3 (R. T. Youker et al., 2009). Interestingly, the C-terminus of VGLUT1 contains a patch of acidic residues that includes two serines, Ser-519 and Ser-522, that are predicted by NetPhos (http://www.cbs.dtu.dk/services/NetPhos/) to be phosphorylated (Fig. 2A). If

phosphorylated by CK2 or another kinase, these residues could form part of a binding site for a PACS family member, allowing indirect binding to APs. However, replacement of these key serine residues with either alanine or aspartate fails to alter the recycling behavior of VGLUT1-pH relative to WT in response to a range of stimulation frequencies (Fig. 2B, C, D). Since it is possible that the presence of the C-terminal dileucine-like motif immediately upstream of these residues could mask any effects of mutation, I examined the recycling of SS/AA and SS/DD mutants combined with the FV/GG mutation. However, no difference is observed between FV/GG SS/AA and FV/GG SS/DD VGLUT1-pH in response to a 30 Hz for 1 min stimulation (Fig. 2E).

The C-terminus of VGLUT1 also contains two polyproline motifs. The more distal motif, PP2, has been shown to bind the endocytic protein endophilin (S. De Gois et al., 2006; J. Vinatier et al., 2006; S. M. Voglmaier et al., 2006). Recent work has suggested that this interaction contributes to functional differences between VGLUT1 and -2 (M. C. Weston et al., 2011). However, little is known about the other polyproline motif, PP1. Since this motif, like PP2, is only found in VGLUT1 and not in VGLUT2 or -3, it is possible that it could be at least partially responsible for functional differences between the VGLUT isoforms. In addition to screening for a protein interactor for PP1 (see Chapter 3), I also examined the effect of PP1 deletion (ΔPP1) on VGLUT1 recycling. No difference is observed between ΔPP1 and WT VGLUT1-pH with 5 Hz for 5 min (Fig. 3A), with 30 Hz for 1 min (Fig. 3B), or with 80 Hz for 20 seconds (Fig. 3D) stimulation. To test the possibility that PP1 may play a role earlier in synaptic development, I also examined recycling of ΔPP1 VGLUT1-pH at DIV10 (days *in vitro*) and observe no difference in recycling relative to WT (Fig. 3C). I also tested whether

altered Ca^{2+} could affect ΔPP1 recycling. However, increasing the $CaCl_2$ concentration in the imaging media to 4 mM (up from 2 mM), or decreasing the concentration to 0.5 mM, does not alter ΔPP1 recycling relative to WT (Fig. 3E, F).

A possible role for the PP1 motif is revealed in the context of the FV/GG mutation of the C-terminal dileucine-like motif. As described in Chapter 2, deletion of the distal C-terminus of VGLUT1 (FV/GG ΔPP) does not result in further disruption of VGLUT1's synaptic targeting. Intriguingly, closer inspection reveals that endocytosis of FV/GG ΔPP is slightly improved over FV/GG (Fig. 4B). This effect appears to be partially replicated by deletion of PP1 (ΔPP1) alone but not deletion of PP2 (ΔPP2). Further mutational analysis reveals that the effect of ΔPP maps to the putative WW domain binding site, PPxY, at the end of PP1 (Fig. 4C). Mutation of Tyr-541 appears to be required for this effect since FV/GG PAXA and FV/GG SYGAT both replicate the endocytic improvement observed with FV/GG ΔPP.

Discussion

While mutation of the serine residues in VGLUT1's C-terminus had no detectable effect under the conditions tested, these residues may serve functions that the present experiments are unable to detect. One possibility is that subtle effects mediated by the serine residues may not easily be seen in the complex environment of VGLUT1 recycling. VGLUT1 has, in addition to the conserved C-terminal dileucine-like motif, two N-terminal dileucine-like motifs and two polyproline motifs (PP1, PP2). At least in the case of the serine upstream of the acidic residues in the dileucine-like motif (Ser-

504), it may easier to detect an effect of this mutation on VGLUT2 recycling. Unfortunately, this approach is not available for the serines that form part of the putative PACS binding site (Ser-519 and Ser-522) since these residues are not conserved in VGLUT2 or -3. It is also possible that the serine residues alter VGLUT1 recycling under conditions that were not tested. For example, the serine residues may only have an effect on spontaneous release or have an effect earlier in development (i.e. DIV10). In the case of the serine immediately upstream of the dileucine-like motif (Ser-504), the effect is likely on size of the readily releasable pool since this is the difference that is observed with the analogous mutation in VGAT.

As to PP1, one possible function for the motif is to direct VGLUT1 towards one endocytic pathway and away from another. The other polyproline motif, PP2, appears to do something similar, directing VGLUT1 towards a fast AP-2 dependent pathway and away from a slower AP-1/3 pathway (S. M. Voglmaier et al., 2006). If this is the case, one reason that no effect is observed with PP1 deletion could be that PP1 directs VGLUT1 towards a pathway that the transporter is already defaulting to under the current culture conditions. However, the FV/GG mutant reveals a function for PP1, specifically for the PPxY motif at the end of the sequence. One interpretation of the fact that mutation of PPxY improves FV/GG endocytosis is that the protein that interacts with PPxY (potentially AIP4 or Nedd4, see Chapter 3) directs VGLUT1 towards an endocytic pathway that is dependent on the FV motif. When the FV motif is disrupted by mutation, the PPxY interaction is still attempting to direct VGLUT1 to this, now non-functional, pathway. Mutation of PPxY then disrupts this interaction and allows VGLUT1 to more easily enter an endocytic pathway that is still functional, presumably one mediated by the

N-terminal dileucine-like motifs. However, additional work is required to validate, or disapprove, this hypothesis.

References

De Gois S, Jeanclos E, Morris M, Grewal S, Varoqui H, Erickson JD (2006) Identification of endophilins 1 and 3 as selective binding partners for VGLUT1 and their co-localization in neocortical glutamatergic synapses: implications for vesicular glutamate transporter trafficking and excitatory vesicle formation. Cell Mol Neurobiol 26:679-693.

Kelly BT, McCoy AJ, Spate K, Miller SE, Evans PR, Honing S, Owen DJ (2008) A structural explanation for the binding of endocytic dileucine motifs by the AP2 complex. Nature 456:976-979.

Vinatier J, Herzog E, Plamont MA, Wojcik SM, Schmidt A, Brose N, Daviet L, El Mestikawy S, Giros B (2006) Interaction between the vesicular glutamate transporter type 1 and endophilin A1, a protein essential for endocytosis. J Neurochem 97:1111-1125.

Voglmaier SM, Kam K, Yang H, Fortin DL, Hua Z, Nicoll RA, Edwards RH (2006) Distinct endocytic pathways control the rate and extent of synaptic vesicle protein recycling. Neuron 51:71-84.

Weston MC, Nehring RB, Wojcik SM, Rosenmund C (2011) Interplay between VGLUT isoforms and endophilin A1 regulates neurotransmitter release and short-term plasticity. Neuron 69:1147-1159.

Youker RT, Shinde U, Day R, Thomas G (2009) At the crossroads of homoeostasis and disease: roles of the PACS proteins in membrane traffic and apoptosis. Biochem J 421:1-15.

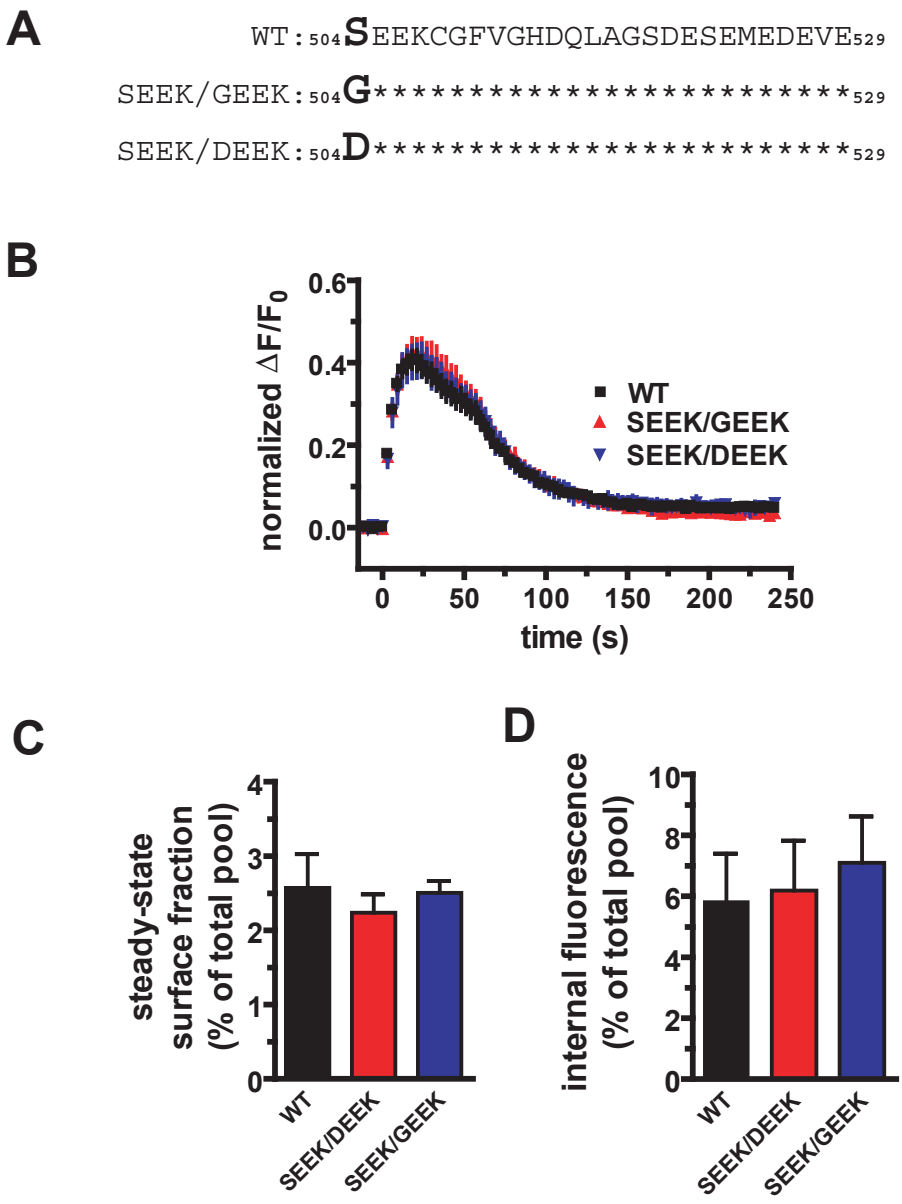
A
WT: 504SEEKCGFVGHDQLAGSDESEMEDEVE529
SEEK/GEEK: 504G*************************529
SEEK/DEEK: 504D*************************529
B
normalized ΔF/F0
0.6
0.4
0.2
0.0
0
50
100
150
200
250
time (s)
WT
SEEK/GEEK
SEEK/DEEK
C
steady-state surface fraction (% of total pool)
4
3
2
1
0
WT
SEEK/DEEK
SEEK/GEEK
D
internal fluorescence (% of total pool)
10
8
6
4
2
0
WT
SEEK/DEEK
SEEK/GEEK

Figure 1

Figure 1: Mutation of Ser-504 does not alter VGLUT1 recycling.

A, Diagram of mutations made in each construct. Unaltered residues are indicated by '*'.

B, Time course of fluorescence change ($\Delta F/F_0$) in neurons transfected with either WT (black), SEEK/GEEK (red), or SEEK/DEEK (blue) VGLUT1-pH in response to 30 Hz for 1 min stimulation (black bar). No difference in recycling is observed with either mutant. Traces from individual synapses were normalized to peak fluorescence reached during stimulation and then averaged. Data are mean ± SEM of 7-9 coverslips from 3 independent cultures with > 20 boutons analyzed per coverslip.

C, The steady-state surface fraction of transporter was unaltered, relative to WT, by either mutation. The fraction was calculated by subtracting fluorescence in pH 5.5 Tyrode's solution from the fluorescence at pH 7.4 prior to stimulation. Data shown as fraction of the total pool of transporter, as revealed by application of NH_4Cl.

D, The total internal fluorescence at rest, as determined by the fluorescence that was not quenched by pH 5.5 Tyrode's. Data shown as fraction of the total pool of transporter, as revealed by application of NH_4Cl.

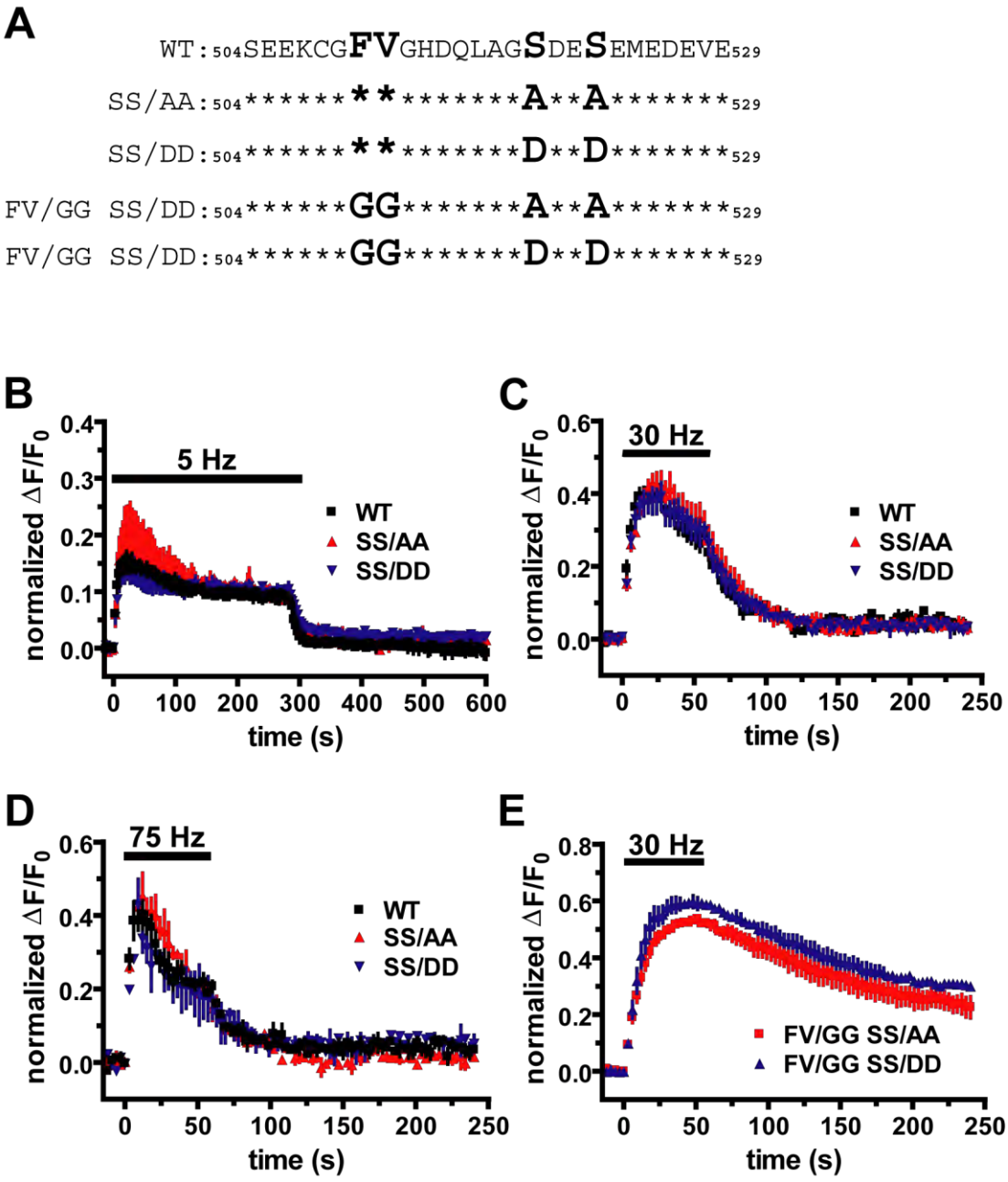
A
WT: 504SEEKCGFVGHDQLAGSDESEMEDEVE529
SS/AA: 504**************A**A*******529
SS/DD: 504**************D**D*******529
FV/GG SS/DD: 504******GG******A**A*******529
FV/GG SS/DD: 504******GG******D**D*******529
B
5 Hz
normalized ΔF/F0
time (s)
WT
SS/AA
SS/DD
C
30 Hz
normalized ΔF/F0
time (s)
WT
SS/AA
SS/DD
D
75 Hz
normalized ΔF/F0
time (s)
WT
SS/AA
SS/DD
E
30 Hz
normalized ΔF/F0
time (s)
FV/GG SS/AA
FV/GG SS/DD

Figure 2

Figure 2: Disruption of Ser-519 and Ser-522 does not alter VGLUT1 recycling.

A, Diagram of mutations made in each construct. Unaltered residues are indicated by '*'.

B, **C**, **D**, Time course of fluorescence change ($\Delta F/F_0$) in neurons transfected with either WT (black), SS/AA (red), SS/DD (blue) VGLUT1-pH in response to 5 Hz for 5 min (**B**), 30 Hz for 1min (**C**), or 75 Hz for 1 min (**D**) stimulation (black bar). Under all stimulation conditions, mutation of Ser-519 and Ser-522 failed to alter recycling of VGLUT1-pH relative to WT. Traces from individual synapses were normalized to peak fluorescence reached during stimulation and then averaged. Data are mean ± SEM of 2-4 coverslips from 1 independent culture with > 14 boutons analyzed per coverslip.

E, Time course of fluorescence change ($\Delta F/F_0$) in neurons transfected with either FV/GG SS/AA (red) or FV/GG SS/DD (blue) VGLUT1-pH in response to 30 Hz for 1 min stimulation (black bar). No difference was observed in the recycling of the two mutants. Traces from individual synapses were normalized to peak fluorescence reached during stimulation and then averaged. Data are mean ± SEM of 2-4 coverslips from 1 independent culture with > 20 boutons analyzed per coverslip.

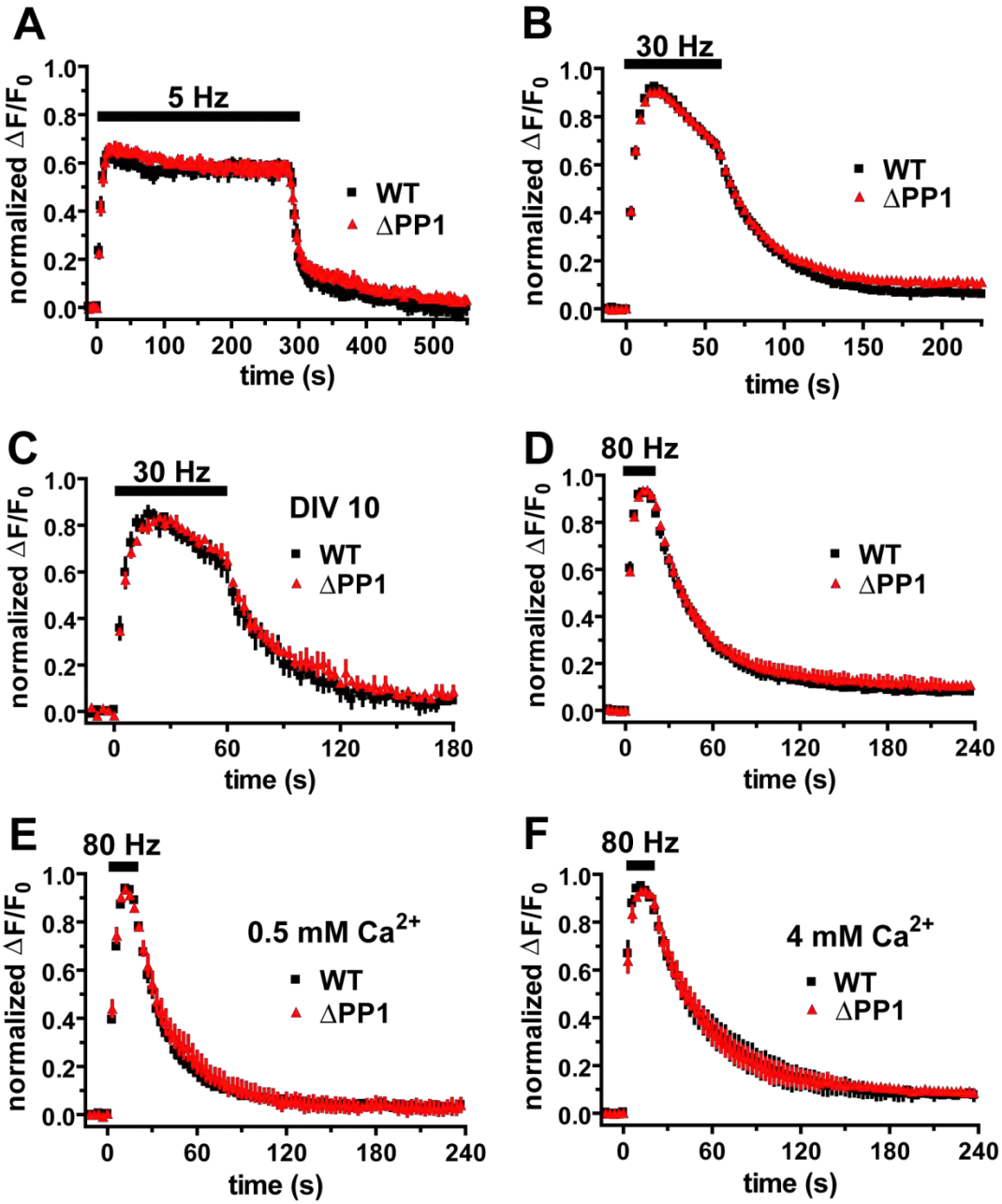
A
5 Hz
WT
ΔPP1
normalized ΔF/F0
time (s)
B
30 Hz
WT
ΔPP1
normalized ΔF/F0
time (s)
C
30 Hz
DIV 10
WT
ΔPP1
normalized ΔF/F0
time (s)
D
80 Hz
WT
ΔPP1
normalized ΔF/F0
time (s)
E
80 Hz
0.5 mM Ca2+
WT
ΔPP1
normalized ΔF/F0
time (s)
F
80 Hz
4 mM Ca2+
WT
ΔPP1
normalized ΔF/F0
time (s)

Figure 3

Figure 3: Deletion of PP1 does not alter VGLUT1 endocytosis.

Time course of fluorescence change ($\Delta F/F_0$) in neurons transfected with either WT (black) or ΔPP1 (red) VGLUT1-pH in response to 5 Hz for 5 min (**A**), 30 Hz for 1 min (**B**, **C**), or 80 Hz for 20 sec (**D**, **E**, **F**) stimulation (black bar). All data were collected from cells at DIV14-17 except data presented in **C** which were collected at DIV10. All data were collected in modified Tyrode's solution with 2 mM $CaCl_2$ with the exception of **E** and **F** where the bath solution $CaCl_2$ concentration was decreased to 0.5 mM or increased to 4 mM, as indicated. No differences in recycling were observed between WT and ΔPP1 VGLUT1-pH under all conditions tested. Traces from individual synapses were normalized to peak fluorescence reached during stimulation and then averaged. Data are mean ± SEM of 5-12 coverslips from at least 2 independent cultures with > 20 boutons analyzed per coverslip except data in **F** which represent 3 coverslips from 1 culture.

A

```
      FV/GG: PPGAPPAPPPSYGATHSTVQPPRPPPP
 FV/GG PAXA: ********A**A****************
 FV/GG PAXY: ********A*******************
FV/GG SYGAT: **********AAA*A*************
 FV/GG ΔPP1: ----------**********************
 FV/GG ΔPP2: ************************-------
```

B

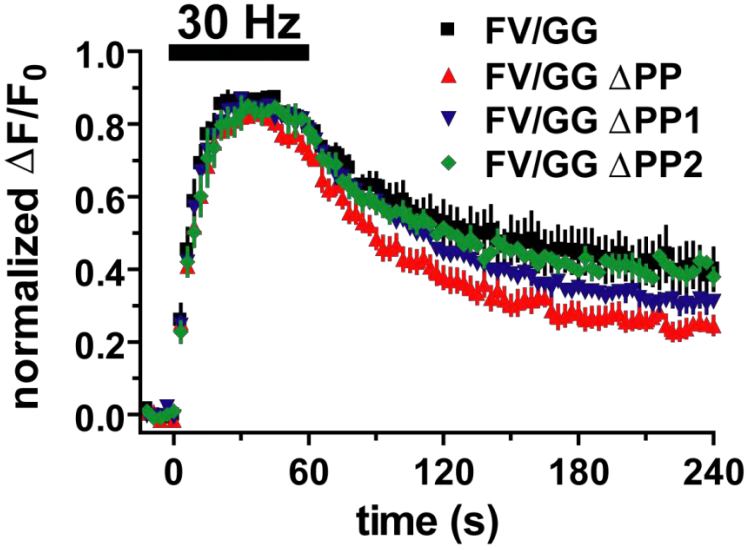

C

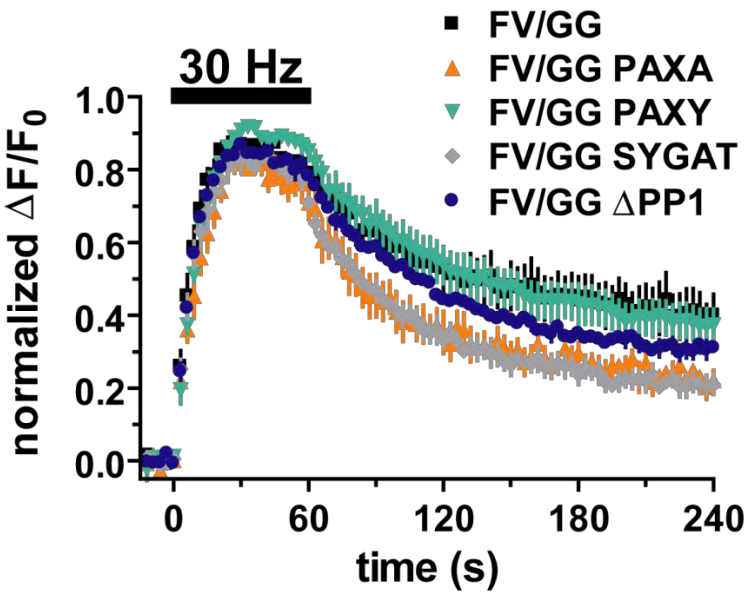

Figure 4

Figure 4: Endocytosis of FV/GG VGLUT1-pH is altered by PPxY motif.

A, Diagram of residues mutated or deleted in various constructs. Residues that were deleted are marked as '-' and unaltered residues are indicated by '*'.

B, Time course of fluorescence change ($\Delta F/F_0$) in neurons transfected with FV/GG (black), FV/GG ΔPP (red), FV/GG ΔPP1 (blue), or FV/GG ΔPP2 (green) VGLUT1-pH in response to 30 Hz for 1 min stimulation (black bar). Traces from individual synapses were normalized to peak fluorescence reached during stimulation and averaged. Elimination of the distal C-terminus (FV/GG ΔPP), by replacement of Pro-531 with a stop codon, improves the efficiency of FV/GG endocytosis. This effect is partially replicated by deletion of PP1 alone (FV/GG ΔPP1). Data are mean ± SEM for 5-11 coverslips from at least 3 independent cultures with > 20 boutons analyzed per coverslip.

C, Time course of fluorescence change ($\Delta F/F_0$) in neurons transfected with FV/GG (black), FV/GG ΔPP1 (blue), FV/GG PAXA (orange), FV/GG PAXY (teal), or FV/GG SYGAT (grey) VGLUT1-pH in response to 30 Hz for 1 min stimulation (black bar). Traces from individual synapses were normalized to peak fluorescence reached during stimulation and averaged. Mutation of Tyr-541, in either the FV/GG PAXA or FV/GG SYGAT, replicates the effect of the full distal C-terminal truncation (FV/GG ΔPP). Only a partial effect is observed with mutation of Pro-539 with the FV/GG PAXY mutant. Data are mean ± SEM for 5-10 coverslips from at least 3 independent cultures with > 20 boutons analyzed per coverslip. FV/GG and FV/GG ΔPP1 traces same as shown in **B**.

Chapter 5:

Conclusions and Future Directions

The work described in this thesis has furthered our understanding of VGLUT1 trafficking and highlighted the complexity of this process. The most significant finding is that VGLUT1 contains three dileucine-like motifs, including two novel N-terminal motifs, which appear to utilize different cellular machinery. I also identified several potential interactors with the PP1 polyproline motif along with a possible function for those proteins. Finally, in the process of screening for PP1 interactors, I identified several potential additional PP2 interactors.

Like all of these findings, the functional implications remain unclear regarding the fact that VGLUT1 contains multiple dileucine-like motifs and that these motifs utilize different mechanisms. The data demonstrating that the C-terminal motif is the dominant endocytic motif and depends upon AP-2 is consistent with central role this particular adaptor is thought to play in endocytosis from the plasma membrane (J. Dittman and T. A. Ryan, 2009; S. H. Kim and T. A. Ryan, 2009; S. J. Royle and L. Lagnado, 2010). In contrast, the functional significance of the N-terminal motifs dependence on AP-1 for targeting VGLUT1 to the recycling pool is unclear. Recent work has suggested that AP-1, along with AP-3, is important in the generation of synaptic vesicles from endosomal intermediates following activity-dependent bulk endocytosis (ABDE) (G. Cheung and M. A. Cousin, 2012). In addition, knockout of a brain-specific AP-1 subunit results in the accumulation of endosomal intermediates in synapses (N. Glyvuk et al., 2010). Thus, one possible explanation is that the N-terminal motifs utilize ABDE and loss of AP-1 inhibits the mutant VGLUT1's ability to re-enter releasable synaptic vesicles, reducing the number that are available for release in response to subsequent stimulation. It is also

possible that the N-terminal motifs are involved in generating synaptic vesicles during development and that this process requires AP-1.

Regardless of the exact functional relevance of this finding, the fact that VGLUT1 has multiple dileucine-like motifs that use different APs, while rare, is not without precedent. One of the small number of proteins with multiple dileucine-like, or tyrosine-based, motifs (S. Storch and T. Braulke, 2001; J. C. Lu et al., 2002; S. Shackleton et al., 2002; S. Radtke et al., 2006; A. Sitaram et al., 2009), the OCA2 protein, a 12-transmembrane domain protein expressed in pigment cells, contains three different dileucine-like motifs. Of the two of these motifs with a known function, one is responsible for trafficking to melanosomes while the other is important for lysosomal targeting. *In vitro* biochemical data suggests that this functional division is due to differential binding to AP-1 and AP-3 (A. Sitaram et al., 2009).

While VGLUT1 trafficking appears to be a highly regulated process that utilizing multiple endocytic pathways, the fundamental question remains as to why this degree of complexity is required. One possible explanation is to prevent plasma membrane expression of VGLUT1. In contrast to the VMATs and VAChT which are driven primarily by the chemical component (ΔpH) of the H^+ electrochemical gradient, negligible at the plasma membrane of most cells, the VGLUTs rely principally on the electrical component ($\Delta\Psi$) (S. Schuldiner et al., 1995; Y. Liu and R. H. Edwards, 1997a). VGLUT on the plasma membrane after exocytosis would be expected to continue transporting cytoplasmic glutamate, in this case out of the cell rather than into secretory vesicles. As a result, the risk of glutamate toxicity may require the tight control of VGLUT surface expression. However, mutation of the conserved dileucine-like C-

terminal motif causes a much stronger effect in VGLUT2 than VGLUT1, suggesting more regulation of VGLUT1 trafficking than VGLUT2. If the risk of glutamate toxicity is the key concern, all glutamatergic cells would be at risk. Alternatively, multiple endocytic motifs may be present on VGLUT1 to ensure that it reaches synapses and is correctly incorporated into synaptic vesicles. However, VGLUT2 is arguably more critical for survival since VGLUT2 is required for respiration, with VGLUT2 null animals dying immediately following birth (A. Wallen-Mackenzie et al., 2006). Finally, both of these explanations would suggest that the presence of the N-terminal motifs in addition to the C-terminal motif is a case of pure redundancy. The differential effects of AP-1 and AP-2 knockdown argue against the sole function of the N-terminal motifs as a 'backup' system for the C-terminal motif, since these findings strongly suggest that the motifs function by non-identical mechanisms and have at least somewhat different functions.

Another possible explanation for the complexity of VGLUT1 trafficking comes from the theory that different endocytic pathways form different synaptic vesicles (S. M. Voglmaier and R. H. Edwards, 2007). If this is the case, regulation of VGLUT1's entry into different endocytic pathways could be a way to alter the functional properties of individual synaptic vesicles and ultimately of the synapse itself. A related possibility is that VGLUT1 can direct, or at least influence, the endocytosis of other synaptic proteins and/or reassembly of synaptic vesicles. In keeping with this idea, synaptic vesicle numbers are reduced in VGLUT1 knockout terminals (R. T. Fremeau, Jr. et al., 2004). Also, dilecuine-like or other trafficking motifs have been identified on all of the classical neurotransmitter transporters found in the CNS but only on a small number of other

synaptic vesicle proteins (H. Fei et al., 2008). However, even if these transporters influence the trafficking of other proteins, they may not be solely responsible for trafficking of all synaptic vesicle components. Recent work has suggested that synaptophysin regulates endocytosis of multiple synaptic vesicle proteins, including VGLUT1, and is necessary for synaptic targeting of synaptobrevin (S. L. Gordon et al., 2011).

Understanding the fine detail of VGLUT1 and -2 trafficking may prove critical to understanding complex neuropsychiatric disorders, such as schizophrenia and autism, which disrupt higher level cognitive thought. For example, the delusions that help define schizophrenia may be caused by impairment in the prefrontal cortex's integration of sensory information from the thalamus with mnemonic information from the hippocampus and cortex (A. Carlsson et al., 1997). Since the thalamic connections are VGLUT2 dependent and the hippocampal/cortical information requires VGLUT1, differences in presynaptic function due to the transporters could affect the balance of input to the circuitry of the prefrontal cortex, potentially resulting in confusion or psychosis. Indeed, novel antipsychotics are being developed that target regulation of neurotransmitter release by prefrontal thalamocortical terminals (G. J. Marek et al., 2001; S. T. Patil et al., 2007).

While the work presented in this thesis reveals new complexity in VGLUT1 trafficking, significant work remains to be completed. The largest task is to further characterize the pathways that the dileucine-like motifs utilize and to understand how the polyproline motifs influence pathway selection.

References

Carlsson A, Hansson LO, Waters N, Carlsson ML (1997) Neurotransmitter aberrations in schizophrenia: new perspectives and therapeutic implications. Life Sci 61:75-94.

Cheung G, Cousin MA (2012) Adaptor protein complexes 1 and 3 are essential for generation of synaptic vesicles from activity-dependent bulk endosomes. J Neurosci 32:6014-6023.

Dittman J, Ryan TA (2009) Molecular circuitry of endocytosis at nerve terminals. Annu Rev Cell Dev Biol 25:133-160.

Fei H, Grygoruk A, Brooks ES, Chen A, Krantz DE (2008) Trafficking of vesicular neurotransmitter transporters. Traffic 9:1425-1436.

Fremeau RT, Jr., Kam K, Qureshi T, Johnson J, Copenhagen DR, Storm-Mathisen J, Chaudhry FA, Nicoll RA, Edwards RH (2004) Vesicular glutamate transporters 1 and 2 target to functionally distinct synaptic release sites. Science 304:1815-1819.

Glyvuk N, Tsytsyura Y, Geumann C, D'Hooge R, Huve J, Kratzke M, Baltes J, Boening D, Klingauf J, Schu P (2010) AP-1/sigma1B-adaptin mediates endosomal synaptic vesicle recycling, learning and memory. EMBO J 29:1318-1330.

Gordon SL, Leube RE, Cousin MA (2011) Synaptophysin is required for synaptobrevin retrieval during synaptic vesicle endocytosis. J Neurosci 31:14032-14036.

Kim SH, Ryan TA (2009) Synaptic vesicle recycling at CNS snapses without AP-2. J Neurosci 29:3865-3874.

Liu Y, Edwards RH (1997a) The role of vesicular transport proteins in synaptic transmission and neural degeneration. Ann Rev Neurosci 20:125-156.

Lu JC, Scott P, Strous GJ, Schuler LA (2002) Multiple internalization motifs differentially used by prolactin receptor isoforms mediate similar endocytic pathways. Mol Endocrinol 16:2515-2527.

Marek GJ, Wright RA, Gewirtz JC, Schoepp DD (2001) A major role for thalamocortical afferents in serotonergic hallucinogen receptor function in the rat neocortex. Neuroscience 105:379-392.

Patil ST, Zhang L, Martenyi F, Lowe SL, Jackson KA, Andreev BV, Avedisova AS, Bardenstein LM, Gurovich IY, Morozova MA, Mosolov SN, Neznanov NG, Reznik AM, Smulevich AB, Tochilov VA, Johnson BG, Monn JA, Schoepp DD (2007) Activation of mGlu2/3 receptors as a new approach to treat schizophrenia: a randomized Phase 2 clinical trial. Nat Med 13:1102-1107.

Radtke S, Jorissen A, de Leur HS, Heinrich PC, Behrmann I (2006) Three dileucine-like motifs within the interbox1/2 region of the human oncostatin M receptor prevent efficient surface expression in the absence of an associated Janus kinase. J Biol Chem 281:4024-4034.

Royle SJ, Lagnado L (2010) Clathrin-mediated endocytosis at the synaptic terminal: bridging the gap between physiology and molecules. Traffic 11:1489-1497.

Schuldiner S, Shirvan A, Linial M (1995) Vesicular neurotransmitter transporters: from bacteria to humans. Physiol Rev 75:369-392.

Shackleton S, Hamer I, Foti M, Zumwald N, Maeder C, Carpentier JL (2002) Role of two dileucine-like motifs in insulin receptor anchoring to microvilli. J Biol Chem 277:43631-43637.

Sitaram A, Piccirillo R, Palmisano I, Harper DC, Dell'Angelica EC, Schiaffino MV, Marks MS (2009) Localization to mature melanosomes by virtue of cytoplasmic dileucine motifs is required for human OCA2 function. Mol Biol Cell 20:1464-1477.

Storch S, Braulke T (2001) Multiple C-terminal motifs of the 46-kDa mannose 6-phosphate receptor tail contribute to efficient binding of medium chains of AP-2 and AP-3. J Biol Chem 276:4298-4303.

Voglmaier SM, Edwards RH (2007) Do different endocytic pathways make different synaptic vesicles? Curr Opin Neurobiol 17:374-380.

Wallen-Mackenzie A, Gezelius H, Thoby-Brisson M, Nygard A, Enjin A, Fujiyama F, Fortin G, Kullander K (2006) Vesicular glutamate transporter 2 is required for central respiratory rhythm generation but not for locomotor central pattern generation. J Neurosci 26:12294-12307.

Publishing Agreement

It is the policy of the University to encourage the distribution of all theses, dissertations, and manuscripts. Copies of all UCSF theses, dissertations, and manuscripts will be routed to the library via the Graduate Division. The library will make all theses, dissertations, and manuscripts accessible to the public and will preserve these to the best of their abilities, in perpetuity.

Please sign the following statement:

I hereby grant permission to the Graduate Division of the University of California, San Francisco to release copies of my thesis, dissertation, or manuscript to the Campus Library to provide access and preservation, in whole or in part, in perpetuity.

Sarah M Fox
Author Signature

12/18/12
Date